PHARMACOLOGIC AND GENETIC ANALYSES OF SPERMIOGENESIS- AND FERTLIZATION-RELATED FACTORS IN *CAENORHABDITIS ELEGANS*

A DISSERTATION

SUBMITTED TO THE COMMITTEE ON

GRADUATE SCHOOL OF SCIENCE AND ENGINEERING IN

SETSUNAN UNIVERSITY

IN PARTIAL FULFILLMENT OF THE REQUIREMENTS FOR

THE DEGREE OF

DOCTOR OF PHILOSOPHY

Tatsuya Tajima

March 2019

I certify that I have read this dissertation and that, in my opinion, it is fully adequate in scope and quality as a dissertation for the degree of Doctor of Philosophy.

Hitoshi Nishimura, Supervisor

I certify that I have read this dissertation and that, in my opinion, it is fully adequate in scope and quality as a dissertation for the degree of Doctor of Philosophy.

Kousaku Murata, Thesis Advisor

I certify that I have read this dissertation and that, in my opinion, it is fully adequate in scope and quality as a dissertation for the degree of Doctor of Philosophy.

Yasumitsu Matsuo, Thesis Advisor

Acknowledgments

First of all, I want to thank Prof. Hitoshi Nishimura, my supervisor, at the Department of Life Science, Faculty of Science and Engineering in Setsunan University. It has been a great honor to me that I am the first Ph.D student in his laboratory. I appreciate his leadership and consistent encouragement.

I extend my thanks to Profs. Kousaku Murata and Yasumitsu Matsuo at the Department of Life Science, Faculty of Science and Engineering in Setsunan University for their helpful comments and suggestions to my Ph.D thesis.

I am also grateful to Prof. Masaaki Omote, Dr. Futa Ogawa and Mr. Masaharu Hashimoto at the Faculty of Pharmaceutical Sciences in Setsunan University for their efforts and spending time to synthesize DDI-1 and its derivatives, key compounds in my study. Prof. Steven W. L'Hernault, Dr. Heather Skye Comstra and Ms. Elizabeth J. Gleason at the Department of Biology in Emory University also provided excellent supports for study of the *C. elegans spe-45* gene.

The present and past members of the Nishimura lab have contributed immensely to my personal and professional time. They have excellently contributed to my work by providing good advice and supports for me. In particular, Mr. Shogo Nakamura, an alumnus of the Nishimura lab, helped me to screen DDI-1 from a chemical library.

Drs. Takeshi Ishihara (Kyushu University), Andrew Fire (Stanford University) and Masaru Okabe (Osaka University) provided pMW118, pPD118.20 and pCXN2 carrying mouse *Izumo1* cDNA, respectively. The *Caenorhabditis* Genetic Center (CGC) and the National BioResource Project (NBRP) provided *C. elegans* strains that were used in my study, and the Drug Discovery Initiative (DDI)/Japan Agency for Medical Research and Development (AMED) provided the Core Library.

Lastly, I would like to thank my parents for all their supports and encouragement. They raised me with a love of science.

Tatsuya Tajima
March 2019

Abbreviations

C. elegans gene/protein names listed below are used in this dissertation without showing full spelling.

aa	amino acid
AEBSF	4-(2-aminoethyl)benzenesulfonyl fluoride
BLAST	basic local alignment search tool
Cas9	CRISPR-associated protein 9
CGC	*Caenorhabditis* Genetic Center
CL	cumulus cell layer
CRISPR	clustered regularly interspaced short palindromic repeat
DAPI	4',6-diamidino-2-phenylindole
DC-STAMP	dendritic cell-specific transmembrane protein
DDI	Drug Discovery Initiative
DIC	differential interference contrast
DMSO	dimethyl sulfoxide
EC	extracellular
EGF	epidermal growth factor
EMS	ethyl methanesulfonate
ERK	extracellular signal-regulated kinase
folt, FOLT	folate transporter family
GLH	germ line helicase

GPI	glycosylphosphatidylinositol
him	high Incidence of males
hSAF	hermaphrodite-derived SAF
IC	Intracellular
Ig	immunoglobulin
IRT	ion-regulated transporter
JNK	c-Jun N-terminal kinase
kgb, KGB	kinase, GLH-binding
L4	fourth larval
LG	linkage group
MAPK	mitogen-activated protein kinase
MEK	MAPK/ERK kinase
MO	membranous organelle
MPK	MAP kinase
mSAF	male-derived SAF
MSP	major sperm protein
NBRP	National BioResource Project
NCBI	National Center for Biotechnology Information
ND	not determined
NGM	nematode growth medium
NS	not significant
PM	plasma membrane

PMK	p38 MAP kinase family
ProK	Proteinase K
Pron	Pronase
PV	perivilelline space
SAF	spermatid-activating factor
SD	standard deviation
SEM	standard error of the mean
sgRNA	single guide RNA
SLC	solute carrier
SM	sperm medium
snf, SNF	sodium: neurotransmitter symporter family
SNP	single nucleotide polymorphism
spe, SPE	defective spermatogenesis
SWM	sperm activation without mating
TEA	triethanolamine
TM	transmembrane
TRPC	transient receptor potential canonical
TRY	trypsin-like protease
zipt, ZIPT	Zrt (ZRT), Irt (IRT)-like protein transporter
ZP	zona pellucida
ZRT	zinc transporter protein

Contents

PART 1

Combined pharmacologic and genetic dissections of spermiogenesis pathways in *C. elegans*

Abstract

C. elegans spermiogenesis involves spermatid activation into amoeboid spermatozoa. Activation occurs through either SPE-8 class dependent or independent pathways. Pronase (Pron) activates the SPE-8 class dependent pathway, whereas no *in vitro* tools are available to stimulate the SPE-8 class independent pathway. Therefore, whether or not there is a functional relationship between these two pathways is currently unclear. In this study, the author found that Proteinase K (ProK) can activate the SPE-8 class independent pathway. *In vitro* spermiogenesis assays using Pron and ProK suggested that SPE-8 class proteins act in the hermaphrodite- and male-dependent spermiogenesis pathways and that some spermatid proteins presumably working downstream of spermiogenesis pathways, including MAP kinases, are preferentially involved in the SPE-8 class dependent pathway. The author screened a library of chemicals, and a compound that was named DDI-1 inhibited both Pron- and ProK-induced spermiogenesis. Surprisingly, several DDI-1 analogs that are structurally similar to DDI-1 blocked Pron-, but not ProK-, induced spermiogenesis. Although the mechanism by which DDI-1 blocks spermiogenesis is yet unknown, the author have begun to address this issue by selecting two DDI-1 resistant mutants. Collectively, the present data support a model in which *C. elegans* male and hermaphrodite spermiogenesis each has its own distinct, parallel pathway.

1-1 Introduction

In many animal species, the formation of fertilization-competent spermatozoa is a complex process that occurs in several different tissues. For example, in mammals (Florman & Fissore, 2015; Nishimura & L'Hernault, 2017), spermatogenesis occurs in the testis and it results in flagellated spermatozoa. During the final phase of spermatogenesis, called spermiogenesis, round spermatids produced by meiosis are transformed into spermatozoa. The initially immotile testicular spermatozoa leave the testis and acquire their motility during passage through the epididymis. After ejaculation, the epididymal spermatozoa become activated and swim from the uterus into the oviduct, where oocytes are fertilized. There are two significant events that encompass activation of mammalian spermatozoa, which are capacitation and the acrosome reaction (Stival et al., 2016). The environments in the male and female sexual organs are indispensable to complete most of those steps, making it challenging to elucidate the molecular basis for how spermatozoa acquire their motility and fertility.

Compared to other species, *Caenorhabditis elegans* has significant advantages for studies of sperm motility and fertility (L'Hernault, 2009; Nishimura & L'Hernault, 2010; Ma et al., 2012; Nishimura & L'Hernault, 2017), because these events naturally occur during spermiogenesis and will also occur in a simple, chemically-defined medium without either hormones or accessory cells. Incubation of *C. elegans* spermatids with spermatid-activating factors (SAFs) stimulates these round, sessile cells to extend pseudopods (instead of flagella),

transforming them into motile spermatozoa (Figure 1.1A-C). Treatment of spermatids with certain, but not all, SAFs results in amoeboid spermatozoa that are competent to fertilize oocytes. *C. elegans* spermatids contain multiple membranous organelles (MOs) (Figure 1.1D), which are secretory vesicles that, collectively, are analogous to the mammalian sperm acrosome (Gleason et al., 2012). Each MO fuses with the plasma membrane (PM) and releases its contents into the extracellular space (Figure 1.1E).

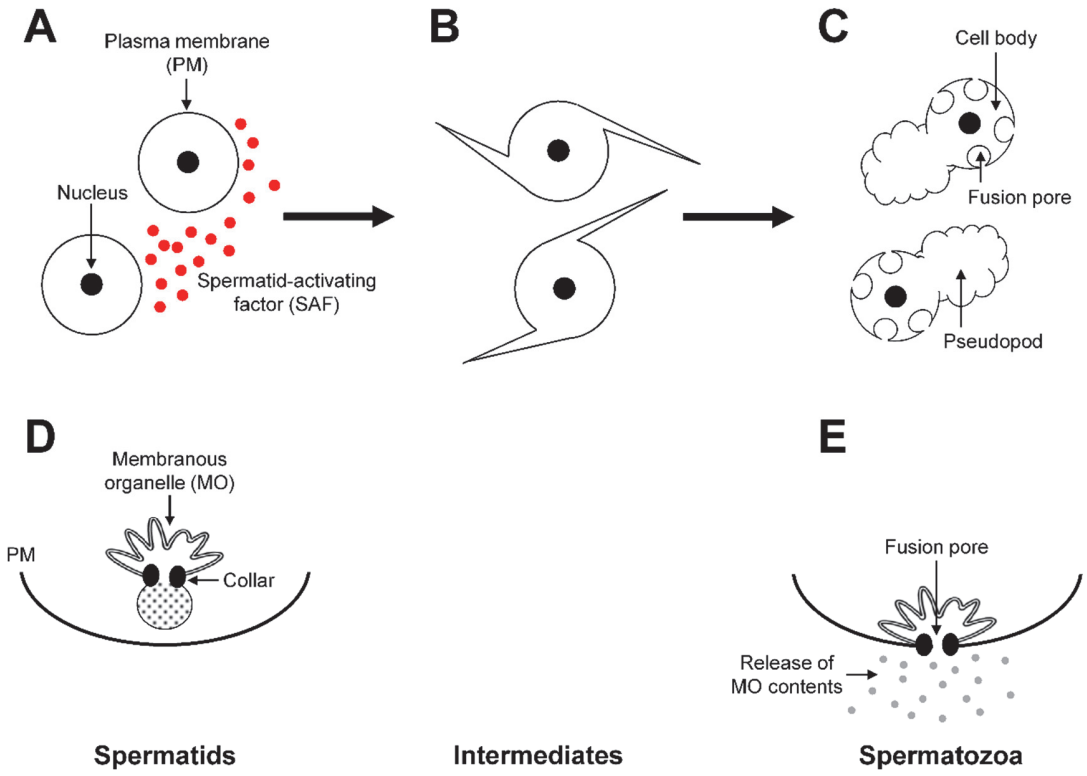

Figure 1.1 Formation and activation of spermatozoa during *C. elegans* spermiogenesis. Sperm formation (A-C) and activation (D, E) are two pivotal processes during *C. elegans* spermatogenesis. (A) Round spermatids are produced *via* meiosis in hermaphrodites and males. (B) Exposure of either hermaphrodite- or male-derived spermatids to activating factors (SAFs) causes them to first transiently extend surface protrusions as they become spermatozoa. (C) The surface protrusions coalesce and a single pseudopod is extended

from the cell body that allows spermatozoa to crawl. (D) Spermatids contain multiple membranous organelles (MOs), which are analogous to the acrosome in mammalian spermatozoa. (E) After spermatids are stimulated with SAFs, the MOs fuse with the plasma membrane (PM) and release their contents into the extracellular space. The MO collars leave a permanent fusion pore in the cell body PM of spermatozoa. Additionally, some SPE-9 class proteins, which are required for gamete fusion, relocate onto the entire sperm surface or the pseudopod surface, where gamete fusion occurs. MO fusion is required for spermatozoa to move properly and to become fertilization-competent.

C. elegans fertilization requires the activity of *spe-9* class genes. One of these genes, *spe-41*/*trp-3* encodes a Ca^{2+}-channel transmembrane (TM) protein that relocates from the MO's to the pseudopodial and cell body surface during MO fusion (Xu & Sternberg, 2003; Takayama & Onami, 2016). In contrast, the SPE-9 TM protein resides in the spermatid PM but translocates to the pseudopodial membrane during spermiogenesis (Zannoni et al., 2003). Relevant to the MO fusion, the acrosome reaction also undergoes the relocation of fusogenic proteins, such as EQUATORIN (Toshimori et al., 1992) and IZUMO1 (Inoue & Wada, 2018), onto the equatorial segment of sperm heads, where spermatozoa fuse with the oocyte PM.

Past genetic studies identified several *C. elegans* genes that are involved in spermiogenesis (L'Hernault, 2009; Nishimura & L'Hernault, 2010). These include the genes that encode SPE-8 (non-receptor type tyrosine kinase) (L'Hernault et al., 1988; Shakes & Ward, 1989; Muhlrad et al., 2014), SPE-12 (single-pass TM protein) (L'Hernault et al., 1988; Shakes & Ward, 1989; Nance et al., 1999), SPE-19 (single-pass TM protein) (Geldziler et al., 2005), SPE-27 (soluble protein) (Minniti et al., 1996), SPE-29 (single-pass TM protein) (Nance

et al., 2000) and SPE-43 (two isoforms, single-pass TM and secreted proteins) (Krauchunas et al., 2018). Mutations affecting any one of these six genes exhibit the same phenotype; hermaphrodites are self-sterile but are cross-fertile after being mated with males carrying the same mutation. The above six proteins are categorized into the SPE-8 class, which define components required for hermaphrodite-dependent spermiogenesis (L'Hernault, 2009; Nishimura & L'Hernault, 2010). Analyses in males have revealed that there is also a male-specific pathway of spermiogenesis that is independent of the SPE-8 class proteins (Smith & Stanfield, 2011; Ellis & Stanfield, 2014).

Table 1.1 *C. elegans* genes involved in spermiogenesis

Gene	LG[1]	M/F[2]	Encoded protein	Sex of mutant in which spermiogenesis does not occur
snf-10	V	15.9	SLC6 transporter (673 aa)	Male
spe-4	I	2.72	Presenilin-like Asp protease (465 aa)	Hermaphrodite and male
spe-6	III	ND	Casein kinase 1-like Ser/Thr kinase (379 aa)	Hermaphrodite and male
spe-8	I	2.92	Non-receptor Tyr kinase with a SH2 domain (512 aa)	Hermaphrodite
spe-12	I	1.20	Single-pass TM protein (255 aa)	Hermaphrodite and partially male
spe-19	V	4.63	Single-pass TM protein (300 aa)	Hermaphrodite
spe-27	IV	9.32	Soluble protein (131 aa)	Hermaphrodite
spe-29	IV	ND	Single-pass TM protein (66 aa)	Hermaphrodite
spe-43	IV	3.97	Soluble protein (226 aa) Single-pass TM protein (273 aa)	Hermaphrodite
spe-46	I	34.5	Six-pass TM protein (290 aa)	Hermaphrodite and male
try-5	V	0.95	Ser protease (327 aa)	Male
zipt-7.1	IV	1.00	Zinc transporter (393 aa)	Hermaphrodite and male

[1]Abbreviations: LG, linkage group; SLC6, solute carrier 6; aa, amino acid; ND, not determined; SH2, src homology 2; TM, transmembrane.

[2]Ratio of gene expression in *fem-3* (male germline-specific) and *fem-1* (female germline-specific) mutant worms, calculated from the data based on previous reports either by Reinke *et al.* (2000) or Reinke *et al.* (2004).

The SPE-8 class dependent pathway is thought to employ a hermaphrodite-derived SAF (hSAF) *in vivo*, but its identity is currently unknown. Studies using spermatids from any of the *spe-8* class mutants demonstrated that the bacterial protease mixture Pronase (Pron) can function as an *in vitro* SAF, but the resulting spermatozoa have multiple spiky surface membrane extensions rather than a single motile pseudopod (Shakes & Ward, 1989; L'Hernault, 2009; Nishimura & L'Hernault, 2010; Ma et al., 2012). Zinc also can activate the pathway *in vitro* (Liu et al., 2013), and the zinc transporter gene *zipt-7.1* is essential for spermiogenesis in both hermaphrodites and males (Zhao et al., 2018). The male-derived SAF (mSAF) functions in the SPE-8 class independent pathway and is likely the serine protease TRY-5 that is found in seminal fluids (Smith & Stanfield, 2011). The *snf-10* gene is also required for male-dependent spermiogenesis and it encodes a solute carrier 6 (SLC6) transporter protein found on the spermatid PM that relocates to the cell body during spermiogenesis (Fenker et al. 2014).

A recent pharmacological study showed that mitogen-activated protein kinases (MAPKs), including extracellular signal-regulated kinase (ERK), c-Jun N-terminal kinase (JNK) and p38, act through Ca^{2+} signaling to regulate *C. elegans* spermiogenesis (Liu et al., 2014). Whether MAPKs are involved in the SPE-8 class dependent or independent pathways or both is currently unclear.

Suppressor screening of *spe-8* class mutants revealed that certain mutations in either of *spe-4* (L'Hernault & Arduengo, 1992; Arduengo et al., 1998; Gosney et al., 2008), *spe-6* (Varkey et al., 1993; Muhlrad & Ward, 2002) or *spe-46* (Liau et al., 2013) genes rescue the self-sterility of *spe-8* class mutants,

suggesting that SPE-4 (presenilin-like aspartic protease), SPE-6 (casein kinase 1-like serine/threonine kinase) and SPE-46 (six-pass TM protein) proteins function downstream of SPE-8 class proteins in hermaphrodite-dependent spermiogenesis. Any of these three suppressor mutations also cause ectopic spermiogenesis in the male gonads. Usually, male-derived spermatids only activate into mature spermatozoa after they are mixed with seminal fluid during ejaculation into the hermaphrodite uterus during mating, so this premature activation occurred despite a lack of competent mSAF. These findings suggested that SPE-4, SPE-6 and SPE-43 prevent precocious activation of spermatids before hSAF or mSAF trigger spermiogenesis and that the SPE-8 class dependent and independent pathways merge together (Figure 1.2).

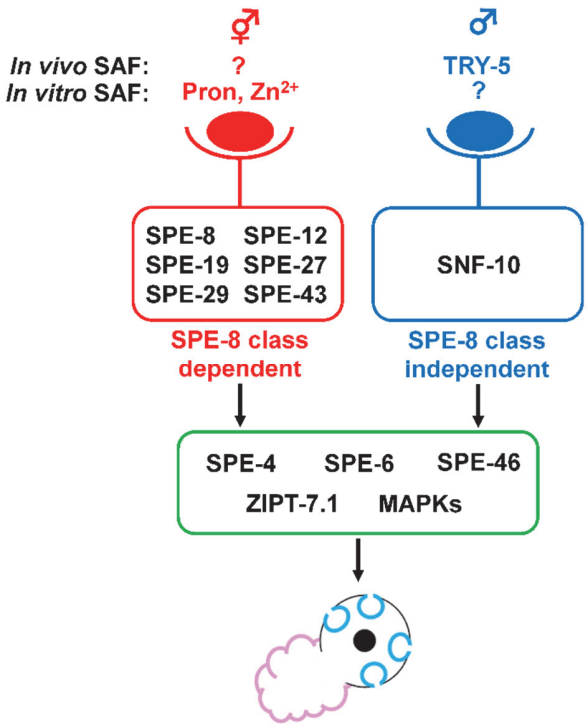

Figure 1.2 A currently proposed model for *C. elegans* spermiogenesis pathways. It has been long thought that *C. elegans* spermiogenesis consists of two pathways that are dependent on and independent of SPE-8 class proteins, each of which are activated *in vivo* by hSAF (unknown) and mSAF (presumably TRY-5), respectively. The SPE-8 class dependent pathway is also known to be activated *in vitro* by Pron or zinc. At either or some points, the SPE-8 class dependent and independent pathways would merge to complete the pseudopod extension (highlighted by a pink line) and the MO fusion (highlighted by cyan

lines). Spermatid proteins which act in the SPE-8 class dependent and independent pathways are surrounded by red and blue rounded rectangles, respectively. Other proteins within the green rounded rectangle are predicted to play roles after the two spermiogenesis pathways merge together.

However, how the SPE-8 class dependent and independent pathways are functionally related to each other and how either pathway elicits pseudopod extension and MO fusion are not well understood. A key piece of information that is currently lacking and might explain this gap is that no *in vitro* SAFs are available that activate the SPE-8 class independent pathway like mSAF. In this study, the author found that Proteinase K (ProK), a bacterial serine protease, can activate the SPE-8 class independent pathway. It was also examined whether ProK and other known SAFs stimulate pseudopod extension (sperm formation) and MO fusion (sperm activation) in various mutant spermatids and whether MAPK inhibitors affect spermatid activation.

These analyses suggested that the *spe-8* class genes are involved in both hermaphrodite- and male-dependent spermiogenesis and that MAPKs are preferentially involved in the Pron- and Zn^{2+}-activated SPE-8 class dependent pathways. A combined pharmacological and genetic approach was taken to further analyze the mechanism of *C. elegans* spermatid activation. First, the author screened a chemical library and discovered that DDI-1 blocks pseudopod extension and partly affects MO fusion during either Pron- or ProK-stimulated spermiogenesis. Second, evaluation of three DDI-1 derivatives showed that they block Pron-induced sperm formation but do not affect ProK-activated spermiogenesis. Lastly, a forward genetic screen was used to isolate two

mutants that produce spermatids capable of undergoing spermiogenesis in the presence of DDI-1. These analyses are most consistent with a new model of *C. elegans* spermiogenesis pathways.

1-2 Results

1-2-1 The SPE-8 class independent pathway related to male-dependent spermiogenesis is activated by ProK

Previous work by others has shown that proteases can participate in spermatid activation both *in vivo* (Smith & Stanfield, 2011) and *in vitro* (Ward et al., 1983). Thus, several additional proteases were tested (data not shown), and it was found that the microbe-derived serine protease ProK can induce spermiogenesis in male-derived spermatids from N2 and *spe-8* class mutants (*spe-8(hc40)*, *spe-12(hc76)*, *spe-19(eb52)* and *spe-27(it110)*) (Figure 1.3). Prior to stimulation with SAF, N2 and *spe-8* class mutant spermatids all exhibited similar round morphology (Figure 1.3A-E). The fluorescent dye FM1-43 (Washington & Ward, 2006) specifically stained the PM of each cell type (Figure 1.3A'-E'), indicating that MO fusion does not occur in spermatids. By incubation with ProK, ~94% of N2 spermatids extended a pseudopod (Figure 1.3F). The pseudopod-bearing cells showed punctate FM1-43 staining at the PM of each cell body (Figure 1.3F'), demonstrating that the MO fusion with the PM occurred. ProK-treatment also caused ~67, ~92, ~45 and ~87% of *spe-8*, *spe-12*, *spe-19* and *spe-27* mutant spermatids to undergo spermiogenesis and become spermatozoa (Figure 1.3G-J,G'-J'). In contrast, Pron, a bacterial protease mixture that is well characterized to activate spermiogenesis in a SPE-8 class-dependent manner (Shakes & Ward, 1989; L'Hernault, 2009; Nishimura & L'Hernault, 2010; Ma et al., 2012), triggered the sperm formation and activation in ~94% of N2 spermatids (Figure 1.3K,K'), but not in *spe-8* (Figure 1.3L,L'), *spe-*

12 (Figure 1.3M,M'), *spe-19* (Figure 1.3N,N') and *spe-27* (Figure 1.3O,O') mutant cells.

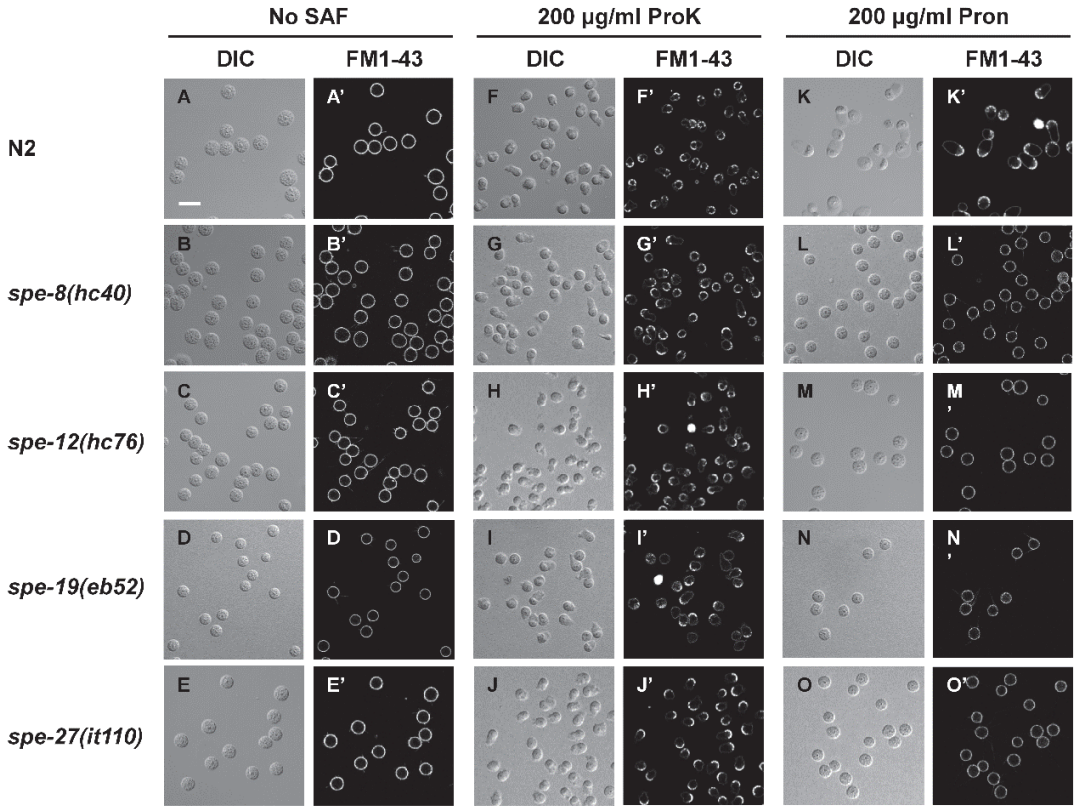

Figure 1.3 Protease-treatment of *spe-8* class mutant spermatids. Spermatids from wild-type (N2), *spe-8(hc40)*, *spe-12(hc76)*, *spe-19(eb52)* and *spe-27(it110)* males were incubated with 200 µg/mL ProK or Pron as a SAF, and then stained with FM1-43. Differential interference contrast (DIC; A-O) and fluorescent (FM1-43; A'-O') images were captured for every examined genotype to observe pseudopod extension and MO fusion. Scale bar, 10 µm.

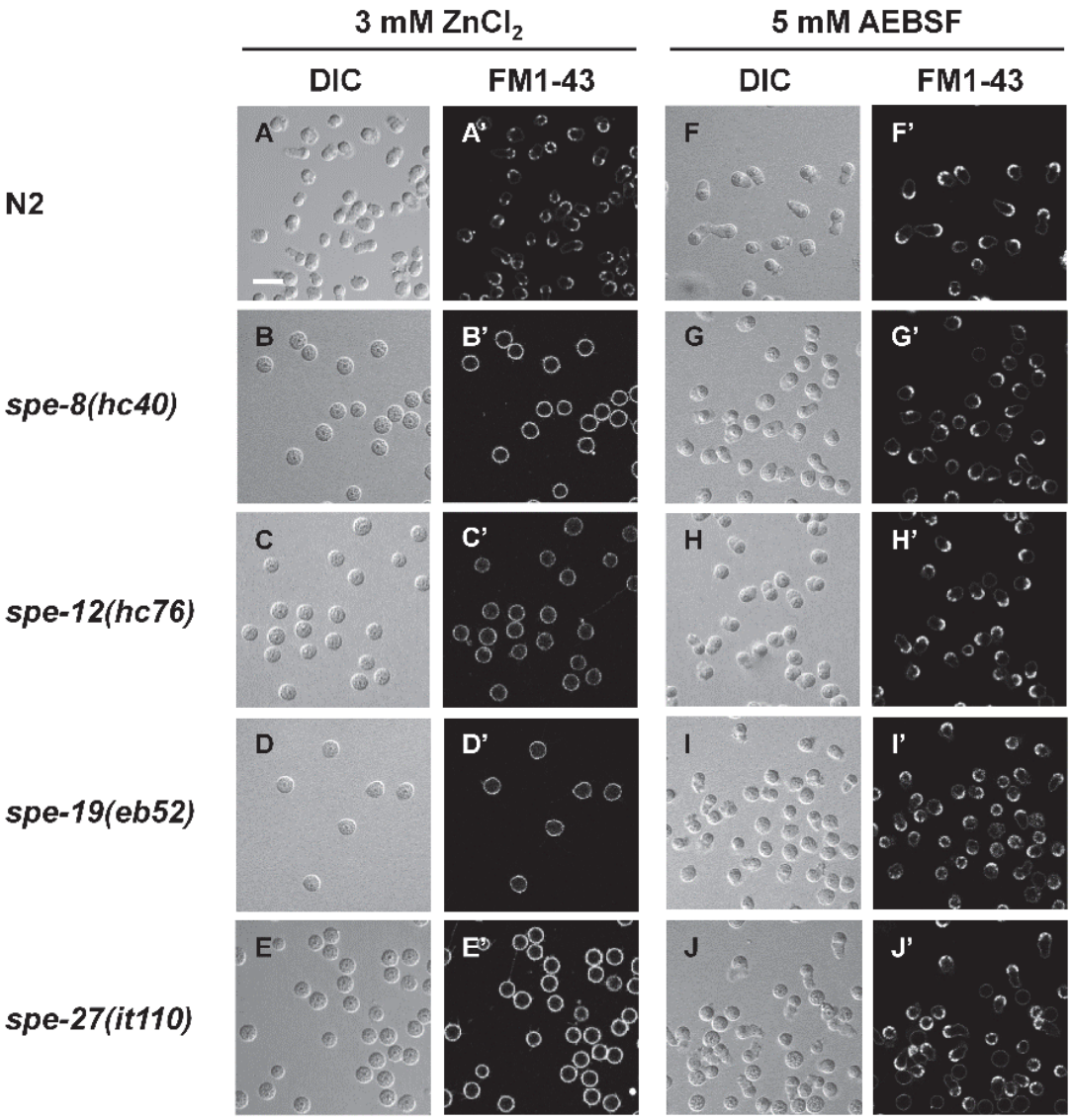

Figure 1.4 Zinc- and MAPK-activation of wild-type and *spe-8* class mutant spermatids. Spermatids were released from N2 (wild type), *spe-8(hc40)*, *spe-12(hc76)*, *spe-19(eb52)* and *spe-27(it110)* males, incubated with 3 mM $ZnCl_2$ or 10 mM 4-(2-aminoethyl)benzenesulfonyl fluoride (AEBSF) to induce spermiogenesis, and then stained with FM1-43. Microscopy was performed as described for Figure 1.3. These data are related to Figure 1.3. Scale bar, 10 μm.

The author employed $ZnCl_2$- and 4-(2-aminoethyl)benzenesulfonyl fluoride (AEBSF)-treatments as control experiments. The labile zinc is known to activate the SPE-8 class dependent pathway (Liu et al., 2013) and exhibited similar effects to those of Pron; Zn^{2+} promoted the pseudopod extension and the MO fusion in ~48% of N2 spermatids (Figure 1.4A,A'), but not in *spe-8* class mutant spermatids (Figure 1.4B-E,B'-E'). AEBSF is an activator of MAPKs (Wijayanti et al., 2005) and it could induce the sperm formation (Figure 1.4F-J) and activation (Figure 1.4F'-J') in both wild type and any of the several *spe-8* class mutant spermatids that were tested. Therefore, ProK showed a novel activity because it could activate *spe-8* class mutant spermatids into spermatozoa that had similar cytology to that of wild type.

1-2-2 SPE-8 class proteins may act in both hermaphrodite- and male-dependent spermiogenesis

It was next examined if the ProK-activated pathway is functionally related to the SLC6 transporter gene *snf-10*, since this gene seems to be involved in male-dependent spermiogenesis (Fenker et al. 2014). When *him-8(e1489)* spermatids (Figure 1.5A,A') were incubated with Pron (Figure 1.5B,B') and ProK (Figure 1.5C,C') as controls, ~83 and ~94% of the cells underwent both the pseudopod extension and the MO fusion, respectively. However, *him-8(e1489); snf-10(hc194)* cells (Figure 1.5F,F') could not respond to either Pron as shown previously (Fenker et al. 2014) (Figure 1.5G,G') or ProK (Figure 1.5H,H'). Thus, both Pron and ProK might activate pathways that are related to male-dependent spermiogenesis.

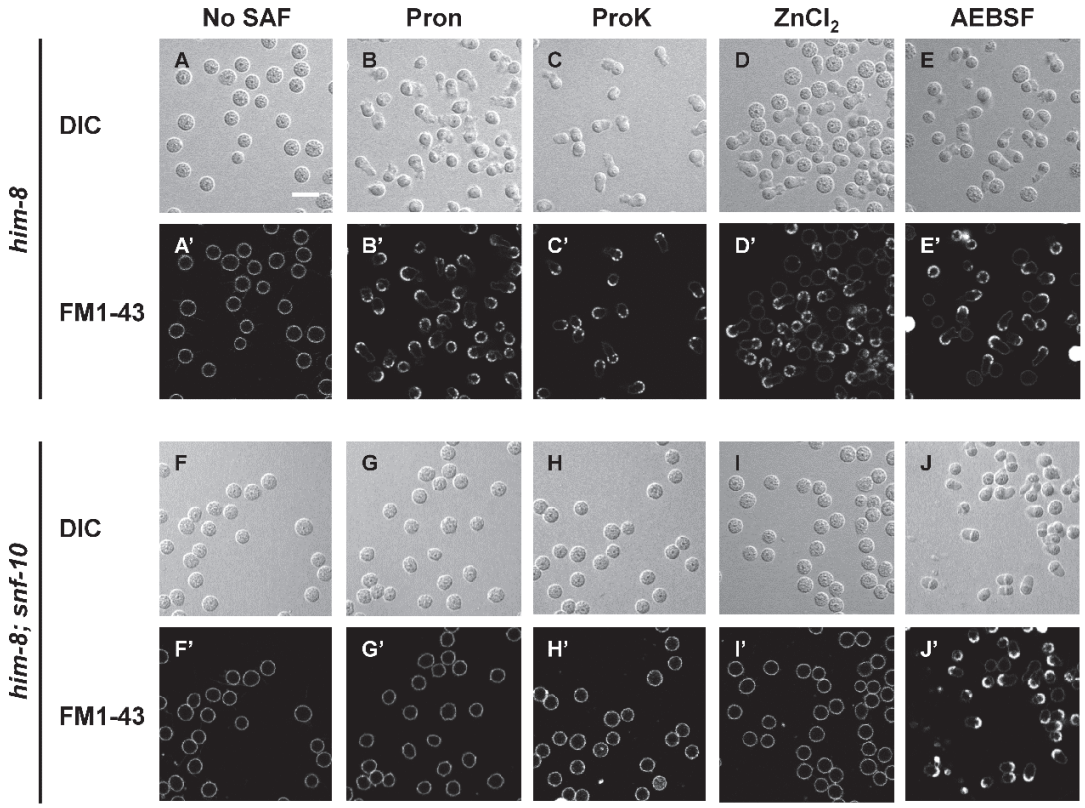

Figure 1.5 Evaluation of the spermiogenesis pathway that is active in males. Spermatids were released from either *him-8(e1489)* or *him-8(e1489); snf-10(hc194)* males, incubated with the indicated SAFs, and then stained with FM1-43. Microscopy was performed as described for Figure 1.3. Scale bar, 10 μm.

$ZnCl_2$, as expected, induced activation of control spermatids into spermatozoa (Figure 1.5D,D'), but did not affect *snf-10* mutant cells after a 20-min incubation (Figure 1.5I,I'). Fenker *et al.* (2014) demonstrated that labile zinc triggers spermiogenesis in the same mutant cells, but several lines of information about the data, such as an incubation period with Zn^{2+}, are unclear in the report. In this study, the *snf-10* mutant spermatids were incubated with the labile zinc for up to ~40 min, after which formation of spermatozoa was

observed at normal levels (data not shown). Thus, *snf-10* mutant spermatids seem to respond to Zn^{2+} more slowly than control cells. AEBSF stimulated *snf-10(hc194)* spermatids (Figure 1.5J,J'), resulting in pseudopod extension and MO fusion occurred at ~74% levels of control spermatids (Figure 1.5E,E'). This result suggests that ERK-, JNK- and/or p38-type MAPKs function downstream of SNF-10.

1-2-3 Intracellular zinc signaling is regulated by MAPKs downstream of SPE-8 class proteins

Spermiogenesis in both sexes requires intracellular zinc signaling that is mediated by the zinc transporter ZIPT-7.1, which appears to function downstream of SPE-8 class proteins (Zhao et al., 2018). The author examined whether Pron and ProK induce spermiogenesis in *zipt-7.1(ok971)* spermatids. *him-5(e1490)* (Figure 1.6A,A') and *zipt-7.1(ok971); him-5(e1490)* (Figure 1.6F,F') spermatids were cytologically indistinguishable. After Pron-treatment, many *zipt-7.1* mutant cells failed to undergo pseudopod extension and MO fusion (~67% levels of control), while the remaining mutant cells had MO fusions but extended abnormally short pseudopods (~33% levels of control) (compare Figure 1.6B,G,B',G'), confirming the prior work by Zhao *et al.* (2018). Surprisingly, ProK induced spermatid activation in many *zipt-7.1* mutant cells (~75% levels of control), and the resulting spermatozoa had pseudopods that were wild type-like in appearance (Figure 1.6C,H,C',H'). These data are challenging to interpret because the ProK-activated pathway does not absolutely require ZIPT-7.1, yet the zinc-transporter partly acts in the SPE-8 class

independent pathway, since a significant number of *zipt-7.1(ok971)* spermatids failed to be activated into spermatozoa by ProK-treatment (~25% levels of control).

$ZnCl_2$ acted as a SAF for control spermatids (Figure 1.6D,D'), but more slowly for the *zipt-7.1* mutant cells (Figure 1.6I,I') (Zhao et al., 2018), indicating that high levels of labile zinc cannot rescue *in vitro* spermiogenesis in the mutant cells. Moreover, AEBSF was capable of inducing spermiogenesis in control spermatids (Figure 1.6E,E'), but incapable in the *zipt-7.1* mutant cells (Figure 1.6J,J'), demonstrating that the activity of ZIPT-7.1 is presumably regulated downstream of MAPKs.

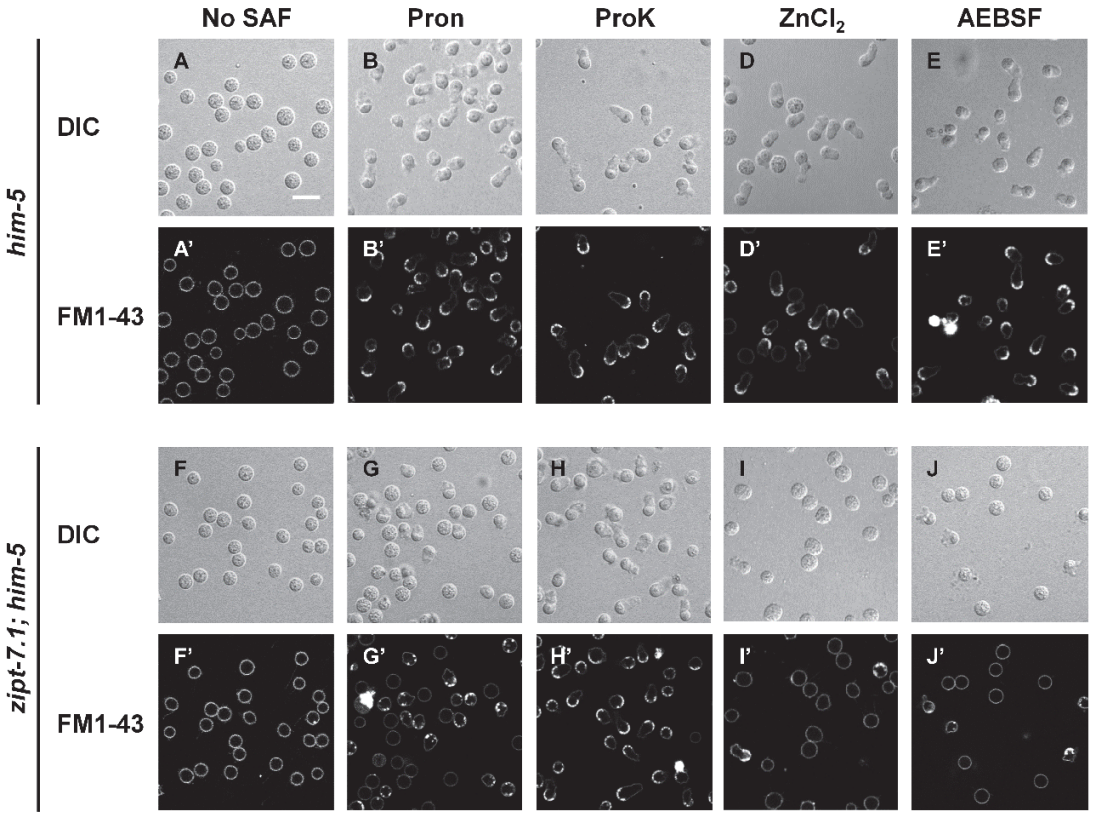

Figure 1.6 Evaluation of the spermiogenesis pathway that is zinc-dependent. Spermatids were released from either *him-5(e1490)* or *zipt-7.1(ok971); him-5(e1490)* males, incubated with the indicated SAFs, and then stained with FM1-43. Microscopy was performed as described for Figure 1.3. Scale bar, 10 μm.

1-2-4 Involvement of MAPKs may be different between the SPE-8 class dependent and independent pathways

Liu *et al.* (2014) showed that MAPK activation is regulated by calcium signaling during *C. elegans* spermiogenesis, and it is likely upstream of the SPE-8 class dependent pathway. This prior work also suggested that downstream signaling molecules, including MAPKs, might participate in both the SPE-8 class dependent and independent pathways. Indeed, consistent with the downstream merging of these two pathways, we showed that activation of MAPKs with AEBSF triggers spermiogenesis in both *spe-8* class (Figure 1.4) and *snf-10* (Figure 1.5) mutant spermatids.

If the “merge” model is true, the SPE-8 class dependent and independent pathways would both utilize the same MAPK(s). We evaluated the effects of several different MAPK inhibitors on wild-type spermatids that were treated with a variety of SAFs (Figure 1.7,1.8). None of the tested MAPK inhibitors exhibited significant effects on spermatids in the absence of SAFs (Figure 1.7A,F,K,P,A’,F’,K’,P’). During Pron-triggered spermiogenesis, inhibitors to MAPK/ERK kinases 1/2 (MEK1/2, activators for ERK1/2) and p38 little affected pseudopod extension and MO fusion (Figure 1.7G,Q,G’,Q’,1.8), whereas the JNK inhibitor dramatically blocked both pseudopod extension and MO fusion, reducing the former by 99% (Figure 1.7L,L’,1.8).

In contrast, ProK-induced spermiogenesis was not substantially affected by either MEK1/2 (Figure 1.7H,H',1.8) or p38 inhibitors (Figure 1.7R,R',1.8). JNK inhibitor only partially blocked pseudopod extension, and ~65% of spermatids could undergo the sperm formation and activation (Figure 1.7M,M',1.8). In this case, unlike the Pron-stimulation in the presence of JNK inhibitor (Figure 1.7L,L'), all spermatids that lacked a normal-looking pseudopod always had unfused MOs (Figure 1.7M,M'). These results suggest that the Pron- and ProK-SAFs interact differently with the process(es) mediated by JNK during spermiogenesis.

When $ZnCl_2$ was used as a SAF, spermiogenesis occurred in the presence of MEK1/2 (Figure 1.7I,I',1.8) and p38 (Figure 1.7S,S',1.8) inhibitors at ~53% and ~82% levels of control, respectively. In contrast, the JNK inhibitor almost completely blocked both pseudopod extension and MO fusion in zinc-treated spermatids (Figure 1.7N,N',1.8). So, while the JNK inhibitor affects Zn^{2+}-mediated spermiogenesis, it is without significant effect on Pron-induced activation, although Pron and zinc both activate the SPE-8 class dependent pathway. These data suggest that the role played by a MAPK depends on the SAF that is activating spermiogenesis.

The ability of AEBSF to induce spermiogenesis was dramatically inhibited in the presence of MEK1/2 (Figure 1.7J,J',1.8) or JNK inhibitors (Figure 1.7O,O',1.8), and partially blocked by a p38 inhibitor (~27% levels of control) (Figure 1.7T,T',1.8). Since AEBSF is an *in vitro* SAF that functions to activate intracellular MAPKs, the present data suggest that ERK and p38 MAPKs play important roles in an as yet unidentified spermiogenesis pathway(s).

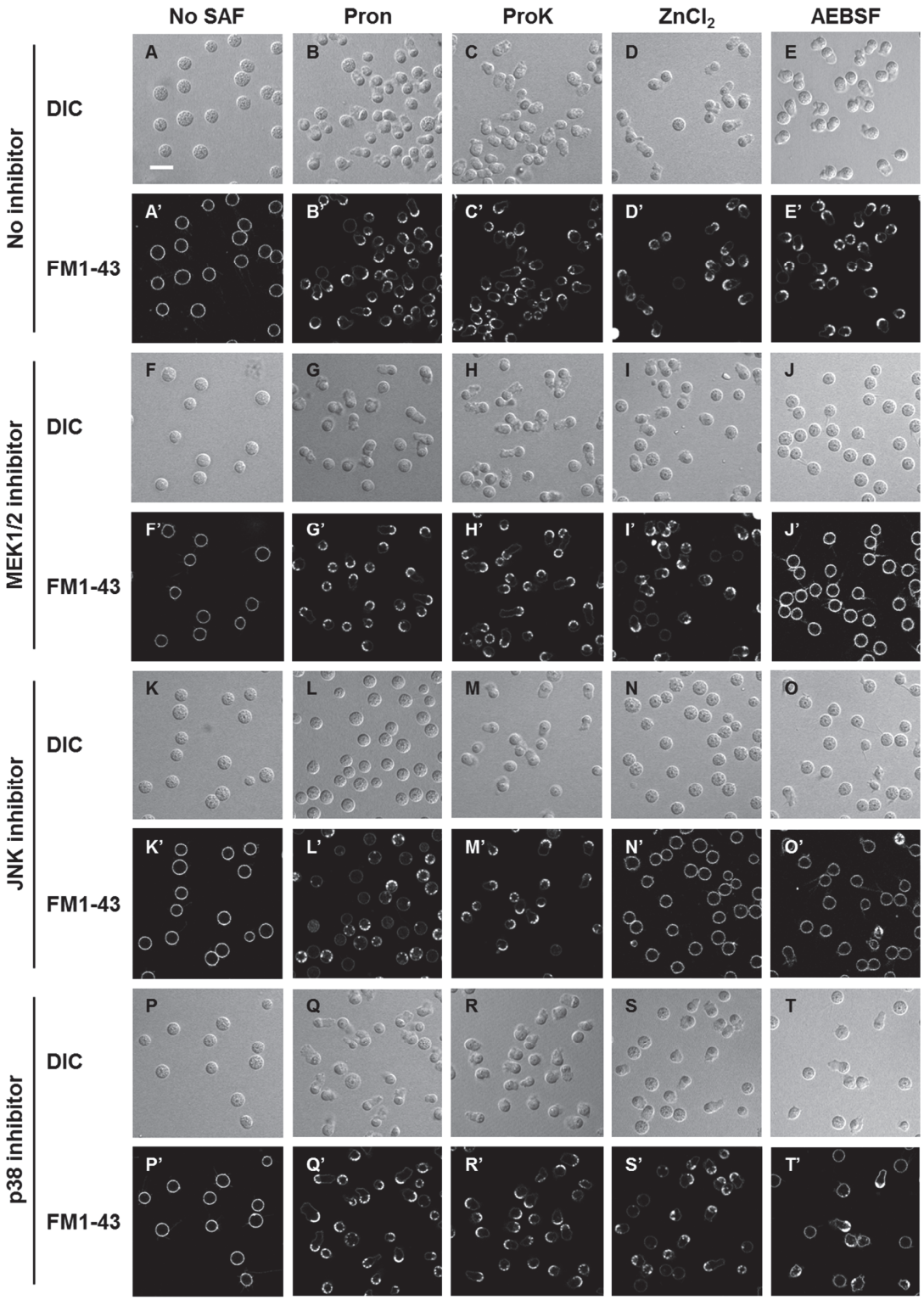
No SAF
Pron
ProK
ZnCl2
AEBSF
No inhibitor
MEK1/2 inhibitor
JNK inhibitor
p38 inhibitor
DIC
FM1-43
A
B
C
D
E
A'
B'
C'
D'
E'
F
G
H
I
J
F'
G'
H'
I'
J'
K
L
M
N
O
K'
L'
M'
N'
O'
P
Q
R
S
T
P'
Q'
R'
S'
T'

Figure 1.7 Effects of MAPK inhibitors on spermiogenesis induced by a variety of SAFs. Spermatids were pre-incubated in media either lacking an inhibitor or containing either MEK1/2, JNK or p38 inhibitors. Spermatids were subsequently treated with the indicated SAFs, and then stained with FM1-43. Microscopy was performed as described for Figure 1.3. Figure 1.8 is based on these data. Scale bar, 10 μm.

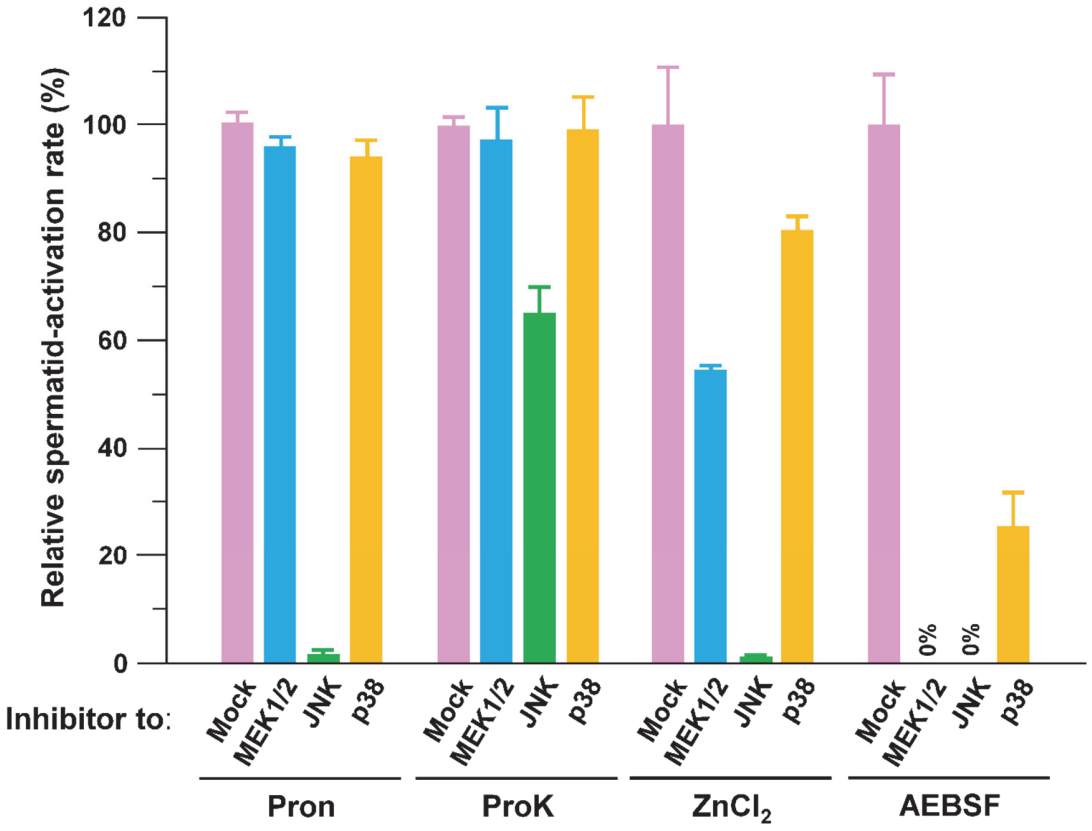

Figure 1.8 Evaluation of the spermiogenesis pathway in which MAPKs participate. After pre-incubation of wild-type spermatids with DMSO (mock) or an inhibitor of either MEK1/2, JNK or p38, the cells were activated with the indicated SAFs and then stained with FM1-43. Microscopy was performed as described for Figure 1.3. Spermatozoon formation rates were calculated by subtracting the number of pseudopod-bearing cells formed by spontaneous activation from those elicited by SAF-treatment. Then, relative spermatozoon formation rates were obtained by assuming that spermatozoon formation rates in the absence of any MAPK inhibitors are 100%. The data shown here are based on

micrographs like those shown in Figure 1.7 and represented as mean ± SD. To calculate the rates represented by each histogram bar, more than 1,000 cells were totally counted in three independent experiments. DMSO, dimethyl sulfoxide; SD, standard deviation.

Like the present work described above, Liu *et al.* (2014) showed that 50 μM U0126 (MEK1/2 inhibitor) prevented ~20% of spermatids from extending pseudopods after Pron-stimulation. When they used the same inhibitor at the concentration of 200 μM, spermatid activation was almost completely disturbed. It is unlikely that higher concentrations of MEK1/2 inhibitor are required to exhibit its inhibitory effect, since our data showed that 50 μM MEK1/2 inhibitor can completely block AEBSF-induced spermiogenesis. The author discovered that the activity of U0126 was affected when spermatids were pre-incubated with the fluorescent dye FM1-43. Therefore, FM1-43 was always added to sperm after incubation with inhibitors and SAFs to avoid any potentially inhibitory effect(s) of FM1-43.

1-2-5 DDI-1 blocks pseudopod extension during C. elegans spermiogenesis

The Drug Discovery Initiative (DDI, at the University of Tokyo, Japan) provides a variety of chemical libraries (www.ddi.u-tokyo.ac.jp). The author screened ~500 compounds that are contained in the DDI Core Library, which consists of ~9,600 entries with divergent structures, and found a compound that interferes with spermiogenesis (named DDI-1 hereafter) (Figure 1.9A,1.10A). In the presence of DDI-1, spermatids exhibited wild type-like cytology (Figure 1.9Bb,b',1.11B,B'). However, during either Pron- or ProK-induced

spermiogenesis, pseudopod extension was completely blocked or brought to arrest at an intermediate stage (Figure 1.9Bf,h,1.11G,L,1.12). Surprisingly, MO fusion occurred in most of the treated cells, even though they lacked appropriately formed pseudopods (Figure 1.9Bf',h',1.11G',L'), indicating that DDI-1 separates these two phenomena that are linked in wild type. DDI-1 showed dose-dependent inhibition, and its 50% inhibitory concentration was ~30 μM towards either Pron- or ProK-induced spermatid activation (data not shown).

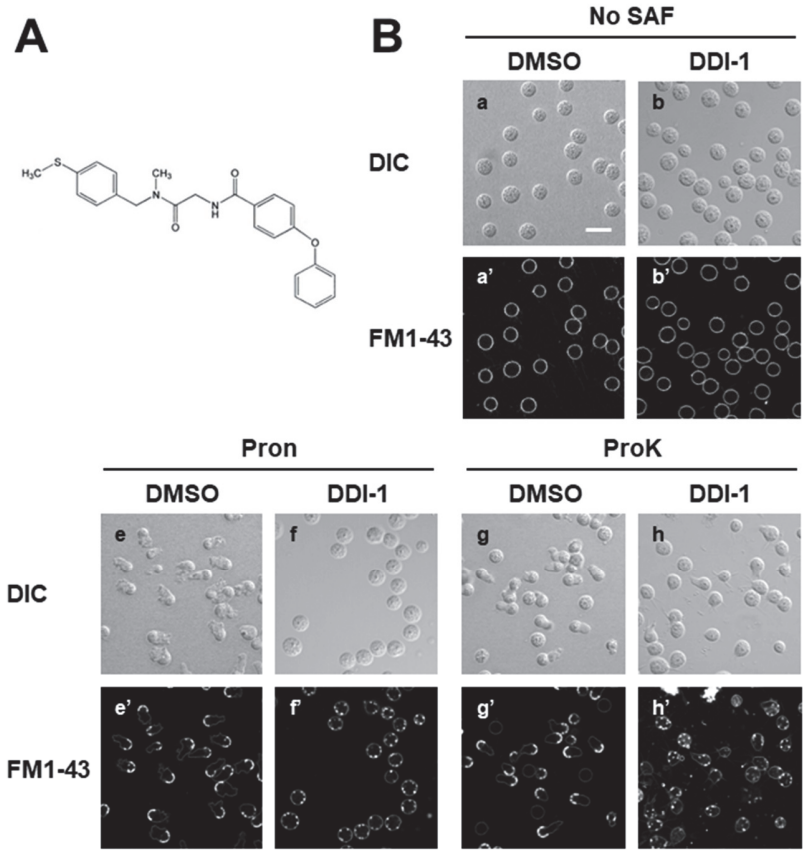

Figure 1.9 The effect of DDI-1 during spermiogenesis. (A) A structure of DDI-1. (B) After pre-incubation of spermatids with DMSO (solvent control) or DDI-1, the cells were

activated with Pron or ProK, and then stained with FM1-43. Microscopy was performed as described for Figure 1.3. Scale bar, 10 μm.

The author synthesized 20 derivatives of DDI-1 and tested their effects on Pron- and ProK-triggered spermiogenesis. DDI-1A (Figure 1.10B), DDI-1C (Figure 1.10C) and DDI-1H (Figure 1.10D) were eventually selected out of the 20 compounds. Like DDI-1, spermatid cytology was unaffected by the presence of either DDI-1A (Figure 1.11C,C'), DDI-1C (Figure 1.11D,D') or DDI-1H (Figure 1.11E,E'). However, any of these DDI-1 derivatives affected Pron-induced spermiogenesis, because most treated cells failed to extend a pseudopod (Figure 1.11H-J,1.12) and fusion of their MOs was partly blocked (Figure 1.11H'-J'). ProK could activate ~17, ~45 and ~36% of spermatids into spermatozoa with normal-appearing pseudopods and MO fusion in the presence of DDI-1A (Figure 1.11M,M',1.12), DDI-1C (Figure 1.11N,N',1.12) and DDI-1H (Figure 1.11O,O',1.12), respectively. On the other hand, DDI-1 and its derivatives all exhibited no significant inhibitory effects on Zn^{2+}-induced spermiogenesis (Figure 1.11Q-T,Q'-T'), while AEBSF-triggered spermiogenesis was completely blocked by those compounds (Figure 1.11V-Y,V'-Y'). These data show that DDI-1 inhibits pseudopod extension after either Pron- or ProK-treatment. DDI-1A, DDI-1C and DDI-1H dramatically inhibits spermiogenesis induced by Pron, but these compounds partially inhibit ProK-induced spermiogenesis. It is also likely that the targets of DDI-1, DDI-1A, DDI-1C and DDI-1H are functionally independent of the Zn^{2+}-pathway and that they are regulated by MAPK signaling.

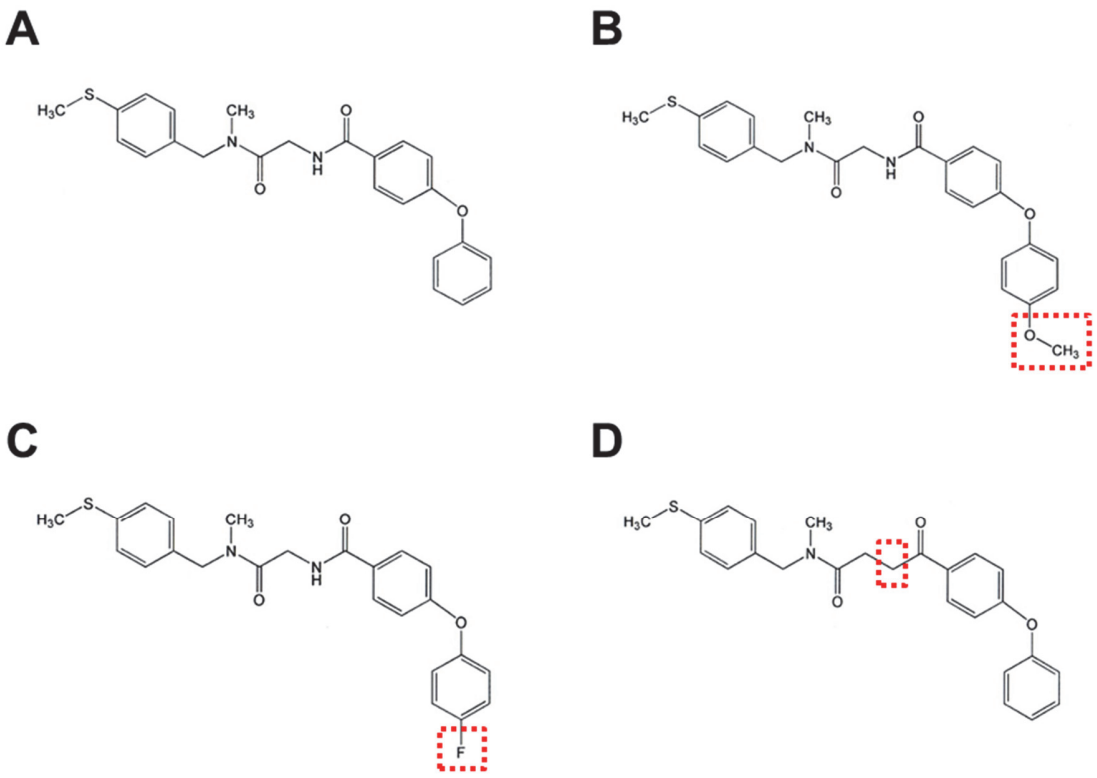

Figure 1.10 Structures of DDI-1 derivatives. Based on the structure of original DDI-1 (A), we synthesized 20 derivatives and examined their effects on Pron- and ProK-induced spermiogenesis. Out of the 20 derivatives, we eventually chose three derivatives, DDI-1A (B), DDI-1C (C) and DDI-1H (D). Squares with red broken lines indicate partial structures that are different from those of DDI-1.

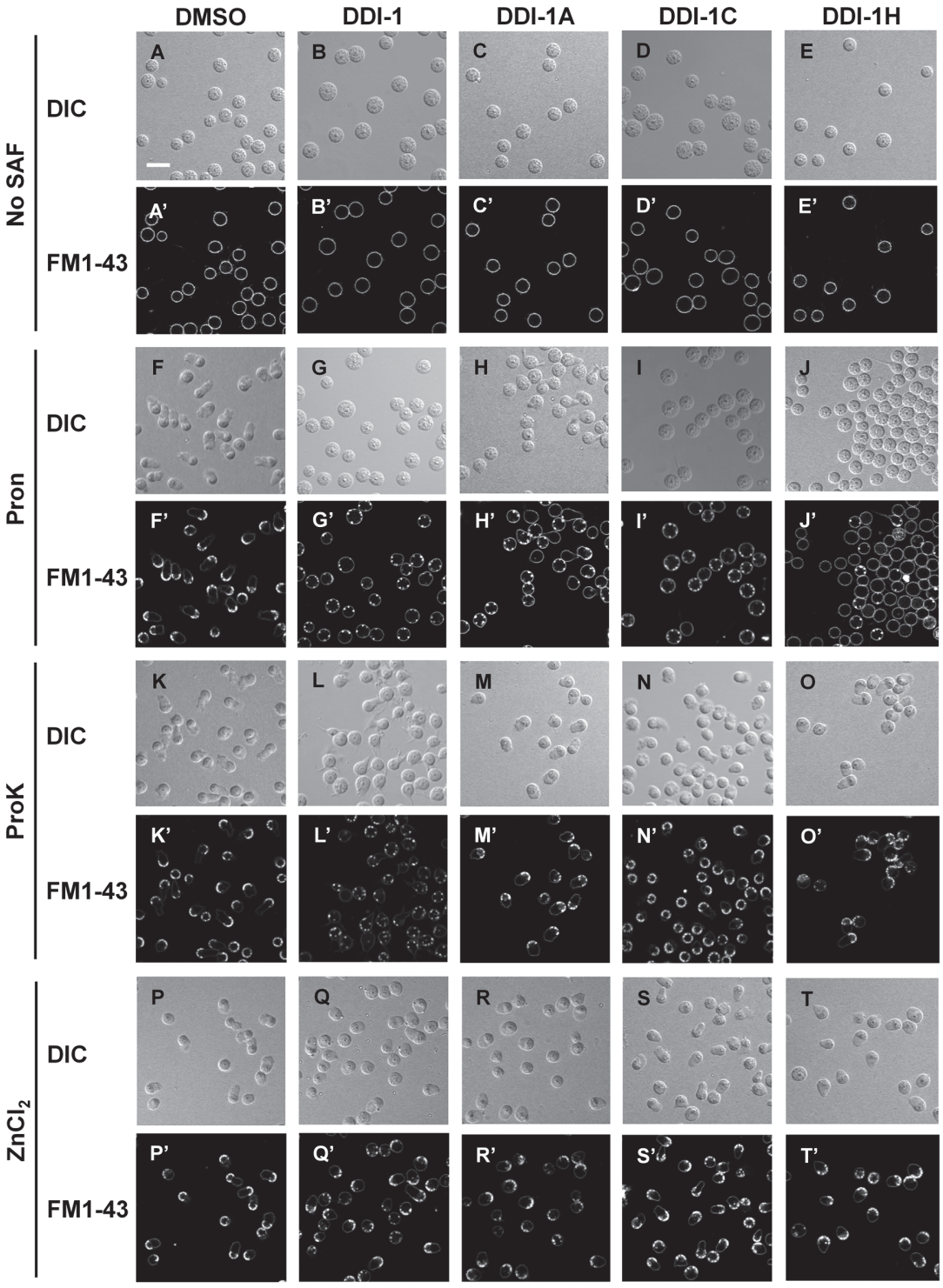

(Figure 1.11, to be continued)

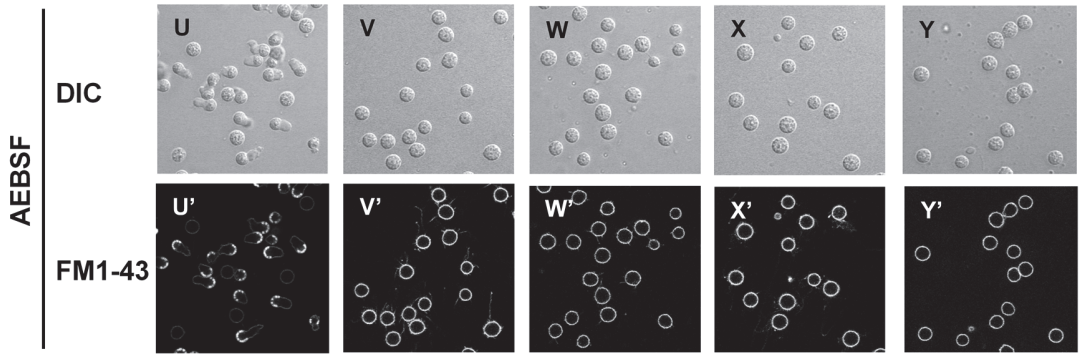

Figure 1.11 Effects of DDI-1 and its derivatives on spermiogenesis induced by a variety of SAFs. After pre-incubation of spermatids with DMSO, DDI-1, DDI-1A, DDI-1C or DDI-1H, the cells were activated with the indicated SAFs, and then stained with FM1-43. Microscopy was performed as described for Figure 1.3. Figure 1.12 is based on these data. Scale bar, 10 μm.

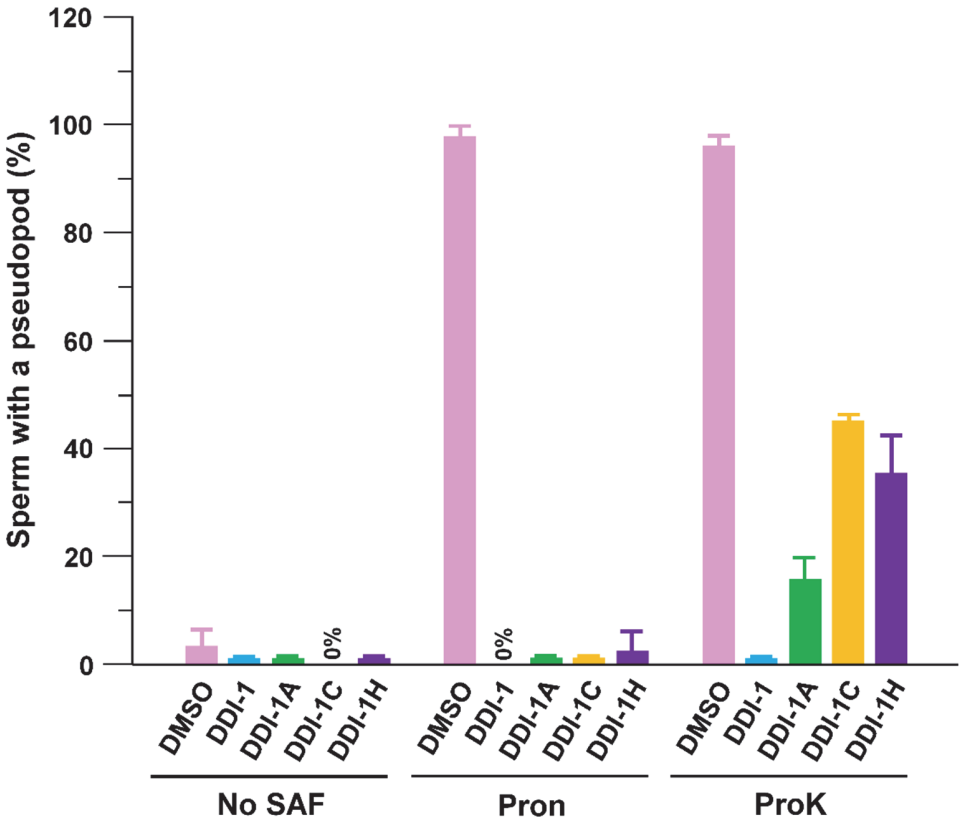

Figure 1.12 The effect of DDI-1 during spermiogenesis depends on the protease SAF. Spermatids were pre-incubated with DMSO (solvent control), DDI-1, DDI-1A, DDI-1C or DDI-1H, activated with the indicated SAFs, and then stained with FM1-43. Microscopy was performed as described for Figure 1.3. The data shown at the vertical axis are ratios of normally-looking spermatozoa among total cells, indicated as mean ± SD (n = 3), and based on those in Figure 1.11. To calculate the ratios, more than 800 cells were totally counted.

1-2-6 Isolation of spermiogenesis mutants that are resistant to DDI-1

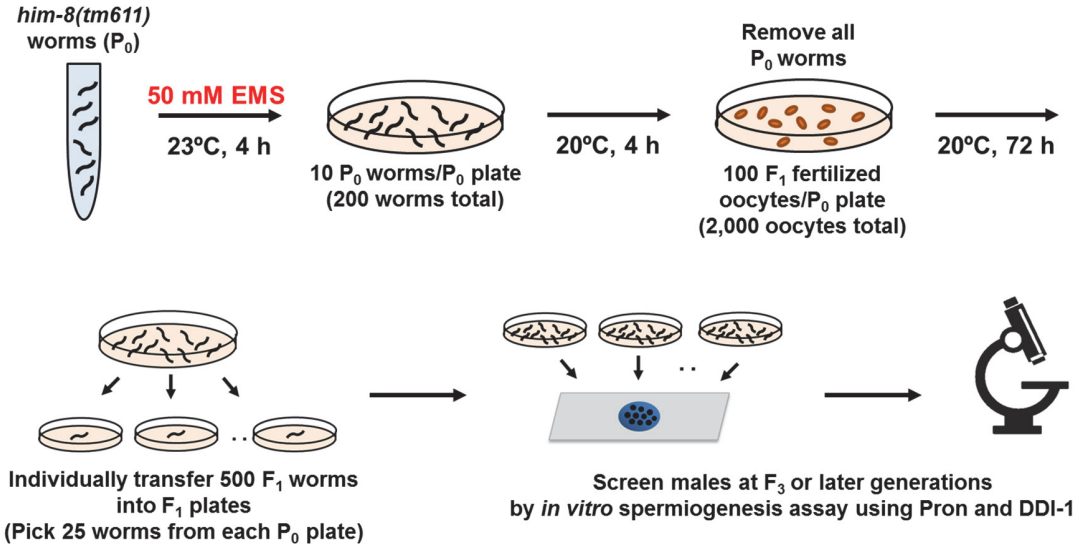

Figure 1.13 Strategy of EMS-mutagenesis to produce DDI-1 resistant worms. This figure summarizes how the author produced and screened *C. elegans* mutants of which spermatids can undergo spermiogenesis by Pron-stimulation in the presence of DDI-1. EMS, ethyl methanesulfonate.

Resistance to DDI-1 requires assaying males, so the author mutagenized *him-8(tm611)* worms, a strain that produces ~40% male self-progeny (www.wormbase.org). As shown in Figure 1.13, after ethyl methanesulfonate (EMS)-treatment of the *him-8* mutant worms (P_0), 200 healthy-looking P_0

hermaphrodites were chosen to put onto plates (10 worms per plate). From each plate, 25 F_1 hermaphrodites were picked to separate plates (500 F_1 worms total). The author screened hermaphrodites at the F_3 or later generations of which tested sons all produced spermatids capable of transforming into spermatozoa by Pron-stimulation even in the presence of DDI-1 (~20 sons were tested per hermaphrodite). Two mutants (temporally named #1-7 and #15-2) that were derived from different P_0 hermaphrodites were eventually recovered.

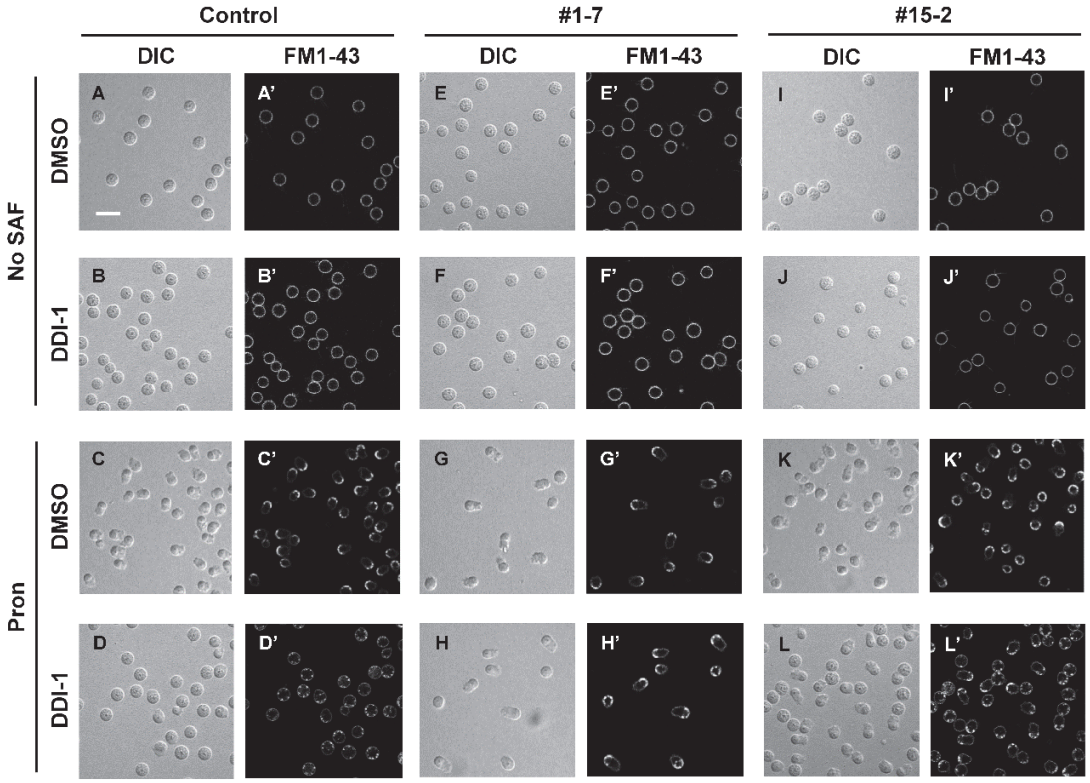

Figure 1.14 Characteristics of mutant spermatids that are DDI-1 resistant. Spermatids from control, #1-7 or #15-2 males were either not treated or treated with Pron and/or DDI-1, and then stained with FM1-43. Microscopy was performed as described for Figure 1.3. Scale bar, 10 μm.

Both #1-7 and #15-2 mutants were self-fertile (data not shown) and produced spermatids with normal cytology in either the absence or presence of DDI-1. After Pron-treatment, spermatids from either #1-7 or #15-2 males could fuse their MOs and extend a wild type-like pseudopod in either the absence (Figure 1.14G,K,G',K') or presence (Figure 1.14H,L,H',L') of DDI-1. In contrast, control spermatids treated with Pron showed MO fusion, but not pseudopod extension, in the presence of DDI-1 (Figure 1.14D,D'). Therefore, spermatid proteins that participate in the DDI-1 inhibitory activity are presumably affected in #1-7 and #15-2 worms. As described above, although these two mutants were derived from different P_0 hermaphrodites, it is currently unclear whether mutant alleles carried by #1-7 and #15-2 worms are the same or different but affect the same gene or affect different genes.

1-3 Discussion

C. elegans spermiogenesis is regulated by the SPE-8 class dependent and independent pathways that correspond to hermaphrodite- and male-dependent spermiogenesis, respectively (L'Hernault, 2009; Nishimura & L'Hernault, 2010; Ellis & Stanfield, 2014). These two pathways both result in the initiation and completion of pseudopod extension and MO fusion. The molecular dissection of the SPE-8 class independent pathway has been challenging, because an array of SAFs and pharmacologic tools have been lacking.

In this study, the author found that ProK is a new tool to explore the SPE-8 class independent pathway (Figure 1.2). This bacterial protease activated all of tested *spe-8* class mutant spermatids. However, the activation rates by ProK varied among the mutants; ~67 and ~45% of *spe-8(hc40)* and *spe-19(eb52)* spermatids transformed into spermatozoa, respectively, while *spe-12(hc76)* and *spe-27(it110)* cells were highly activated at ~92 and ~87% levels, respectively. This implies that a few *spe-8* class genes, such as *spe-8* and *spe-19*, might be also involved in the ProK-induced spermiogenesis pathway. Another possibility is that a difference of the substrate specificities of *in vivo* (presumably TRY-5) and *in vitro* (ProK) SAFs might cause the differential activation rates of *spe-8* class mutant spermatids. ProK is a protease with broad substrate specificity that likely digests numerous spermatid-surface and spermatid-secreted proteins that would likely include the native substrate(s) of TRY-5. Nance *et al.* (1999) suggested that *spe-12* functions in male-dependent spermiogenesis, and this is inconsistent with our observation that ProK could almost completely activate the

spe-12 mutant spermatids into spermatozoa (Figure 1.3). Why this discrepancy exists is unclear, but it might be also based on the highly digestive property of ProK, resulting in rescue of a defect that is caused by the *spe-12* mutation.

It seems probable that ProK-digestion of spermatid proteins results in an extracellular signal(s). Among *in vitro* SAFs that have been so far reported, monensin (cation ionophore) (Nelson & Ward, 1980) and triethanolamine (TEA, weak base) (Ward et al., 1983) can activate *spe-8* class mutant spermatids into spermatozoa like ProK. However, to induce spermiogenesis, monensin and TEA act within spermatids to raise intracellular pH. Whether monensin and TEA play their roles either downstream of the SPE-8 class proteins or at a certain point in the SPE-8 class independent pathway or both is not currently known. Since it is likely that mSAF functions as an extracellular factor that initiates spermiogenesis *in vivo*, ProK is a useful substitution for mSAF to use in *in vitro* experiments.

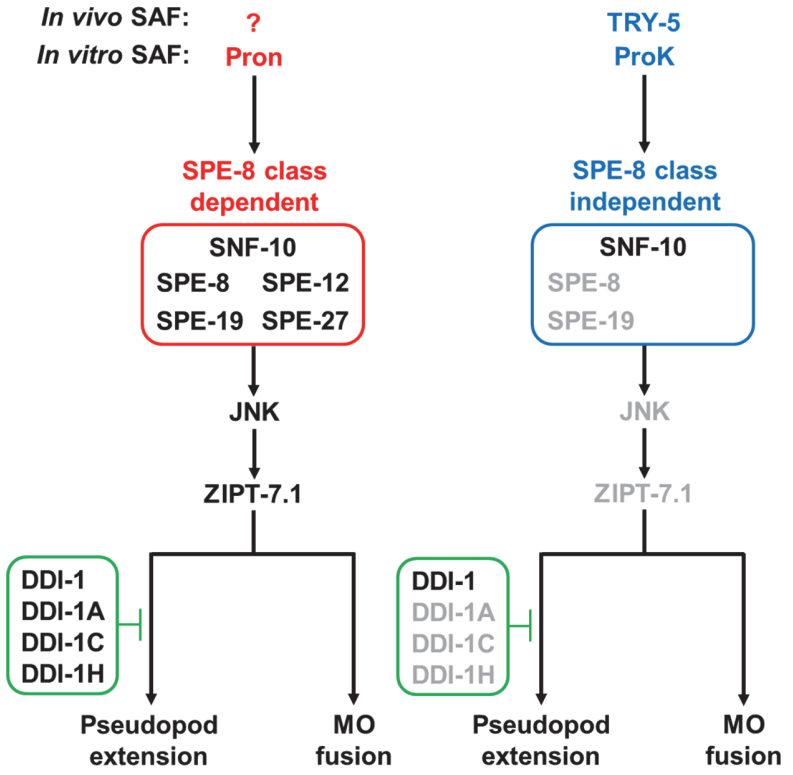

Figure 1.15 A model of *C. elegans* spermiogenesis pathways that are activated by Pron and ProK. How the proteins within the red and blue rounded rectangles act relative to each other are not yet determined. Green rounded rectangles represent compounds of DDI-1 series. Light gray letters show proteins and compounds that likely participate, but not at high levels, in corresponding pathways. Arrows and T-shaped arrows mean reactions of activation and inhibition, respectively.

Male-dependent spermiogenesis was first linked to proteolysis by the discovery of SWM-1. This protein carries two trypsin inhibitor-like domains and prevents ectopic spermiogenesis in the male gonads (Stanfield & Villeneuve, 2006). Indeed, SWM-1 likely inhibits TRY-5 (Smith & Stanfield, 2011), a serine protease that activates male-dependent spermiogenesis as mSAF. Seminal fluids presumably contain another protease SAF for male-dependent spermiogenesis that is blocked by SWM-1. If ProK corresponds to TRY-5, Pron might be an *in vitro* substitution for another mSAF because the Pron-activated pathway seems to be related to male-dependent spermiogenesis (Figure 1.5, also discussed later). Defining whether one or multiple proteases function during spermiogenesis in males is required to elucidate how *in vivo* and *in vitro* SAFs are functionally related to each other.

Genetic and pharmacological analyses in this study have given new insights into *C. elegans* spermiogenesis that allow to propose a new model for spermiogenesis pathways in this animal (Figure 1.15). Such work suggests that the *spe-8* class genes might act in both hermaphrodite- and male-dependent spermiogenesis. As previously reported (Fenker et al., 2014), the author found that *snf-10(hc194)* spermatids do not respond to Pron-stimulation (Figure 1.5G,G'). Male-dependent spermiogenesis is aberrant in *snf-10(hc194)*

mutants, and this probably explains why *snf-10* mutant cells were not activated by ProK-treatment (Figure 1.5H,H'). One plausible interpretation of this fact is that the Pron-activated SPE-8 class dependent pathway corresponds to male-dependent spermiogenesis. Previously, only hermaphrodites were thought to require the *spe-8* class genes during *C. elegans* spermiogenesis, because *spe-8* class mutant males were fertile. Ancestral dioecious nematode species presumably had two redundant pathways for spermiogenesis in males (Baldi et al., 2009; Wei et al., 2014). So, perhaps the SPE-8 class dependent pathway evolved from one that initially functioned exclusively in males to one that functioned primarily, but not exclusively, in hermaphrodites.

$ZnCl_2$ did not activate *snf-10*-null mutant spermatids after 20-min incubation (Figure 1.5I,I'), but prolonged incubation allowed mutant cells to activate into spermatozoa (data not shown). There might be multiple pathways that are activated by zinc, one of which depends on SNF-10, corresponding to male-dependent spermiogenesis. Another pathway is presumably independent from SNF-10, corresponding to hermaphrodite-dependent spermiogenesis, and activated later than the SNF-10 dependent pathway. Indeed, the micronutrient element zinc has been proposed to regulate spermiogenesis in hermaphrodites and males (Liu et al., 2013).

Our analyses of *zipt-7.1(ok971)* spermatid activation (Figure 1.6) lead to a similar interpretation to that proposed for *snf-10(hc194)* cells. The *zipt-7.1* encoded zinc transporter functions during spermiogenesis in both sexes (Zhao et al., 2018). Since ProK can induce spermiogenesis in the *zipt-7.1* mutant cells, this suggests that male-dependent spermiogenesis contains an additional

pathway(s) besides the ProK-induced pathway. As for *snf-10* mutants, perhaps the Pron-induced pathway acts through *spe-8* class genes during male-dependent spermiogenesis.

Previous work suggested that the SPE-8 class dependent and independent spermiogenesis pathways share common downstream signaling, including the MAPK cascade (Liu et al., 2014). Our analyses using MAPK inhibitors (Figure 1.7,1.8) revealed that a JNK inhibitor almost completely blocks spermiogenesis in Pron-treated spermatids, while ProK could activate most spermatids in the presence of JNK inhibitor. Although MEK1/2 and p38 inhibitors had a modest effect on spermiogenesis after Pron- or ProK-treatment of spermatids, these two compounds, like the JNK inhibitor, showed significant inhibitory effects during Zn^{2+}-induced spermiogenesis. These findings suggest that the Pron-, ProK- and Zn^{2+}-spermiogenesis activators utilize different MAPKs and define three distinct pathways.

The author evaluated several MAPK inhibitors, but only the JNK inhibitor caused >95% inhibition of the Pron- and Zn^{2+}-induced pathways, suggesting that JNK plays a pivotal role(s) during spermiogenesis. While such the pharmacological approach is useful, one worries that MAPK inhibitors might not be absolutely specific and/or could depend on cell types that are treated with the drugs. Since the *C. elegans* genome is predicted to encode four JNK-type MAPKs (JNK-1, KGB-1, KGB-2 and C49C3.10) (Andrusiak & Jin, 2016), the author is currently investigating the functions of these JNKs during spermiogenesis, using appropriate mutants. KGB-1 might be intriguing, because *kgb-1* mutant hermaphrodites and males are sterile, but male germ cells

are present in the gonads of both sexes (Smith et al., 2002), implying that *kgb-1* mutant spermatids might not appropriately transform into spermatozoa.

ERK and p38, unlike JNK, might not play their roles in the protease-pathways, but possibly act in the zinc-activated spermiogenesis pathway. Like JNK-type MAPKs, multiple paralogs of ERK (MPK-1 and MPK-2) and p38 (PMK-1, PMK-2 and PMK-3) are encoded in the *C. elegans* genome. The evolutionarily conserved ERK signal transduction pathways regulate a variety of cellular events, including proliferation and differentiation of various cell types, while p38 MAPKs seem to be involved in response to environmental stresses (Roux & Blenis, 2004). Therefore, determining which paralogs of ERK and p38 MAPKs are involved in *C. elegans* spermiogenesis remains as an important goal.

We screened a chemical library and discovered a novel compound (DDI-1) that blocks spermiogenesis (Figure 1.9). This compound blocked pseudopod extension elicited by treatment of spermatids with either Pron or ProK. Three DDI-1 derivatives that we synthesized, DDI-1A, DDI-1C and DDI-H (Figure 1.10), retained this ability to block Pron-stimulated spermiogenesis, but they were without effect on ProK-stimulated spermiogenesis (Figure 1.11,1.12). Perhaps DDI-1 interacts with a target protein(s) in the Pron-pathway and another in the ProK-pathway, while DDI-1A, DDI-1C and DDI-H preferentially bind to a protein(s) that specifically acts in the Pron-pathway. Zn^{2+} seems to act at a different point in the pathway or, perhaps, another pathway, since none of the compounds of the DDI-1 series affected Zn^{2+}-induced spermiogenesis (Figure 1.11,1.12).

So far, attempts in this study to chemically modify DDI-1 so that it can be

attached to beads and used for affinity-purification have been unsuccessful. Consequently, the author searched for and recovered two EMS-induced mutants (#1-7 and #15-2) that were resistant to the effects of DDI-1 as an alternative way to identify the DDI-1 target protein(s). Other than drug-resistance, both of these mutants exhibited no other obvious defects and they had normal self-fertility (data not shown). It is currently investigating whether or not these two mutations suppress or enhance the defects of *spe-8* class, *snf-1*0 and *zipt-7.1* mutants. Moreover, a complementation test, single nucleotide polymorphism (SNP) mapping including chromosomal mapping, and deep genomic sequencing are ongoing to identify the affected genes in #1-7 and #15-2 worms. These two mutants should be quite useful in revealing how pseudopod extension is regulated by the different spermiogenesis pathways that function in *C. elegans*.

1-4 Experimental procedures

1-4-1 Worm strains

The author maintained and cultured worms at 20ºC, unless otherwise stated, according to standard methods reported by Brenner (1974). *C. elegans* var. Bristol (N2), *him-5(e1490)V* (DR466) or *him-8(e1489)IV* (CB1489) worms were used as wild-type/control strains. The following strains were also used in this study: *spe-8(hc40)I* (BA785), *spe-12(hc76)I; him-8(e1489)IV* (CB4951), *spe-19(eb52)V* (AD213), *spe-27(it110)IV* (BA900), *snf-10(hc194)V* (BA1093), *zipt-7.1(ok971)IV* (VC739) and *him-8(tm611)IV* (CA259). All the above strains were obtained from the *Caenorhabditis* Genetic Center (CGC, at the University of Minnesota, USA).

1-4-2 Chemicals and reagents

Pron and AEBSF were purchased from Sigma-Aldrich, ProK from Nacalai (Kyoto, Japan), U0126 (MEK1/2 inhibitor), SP600125 (JNK inhibitor) and SB202190 (p38 inhibitor) from Wako (Osaka, Japan), and FM1-43 from Molecular Probes. Other chemicals that we used were of the highest quality available. The stock solutions 20 mg/ml Pron and 10 mg/ml ProK were prepared in 1 mM HCl, 400 mM AEBSF and 1 mg/ml FM1-43 in water, and 10 mM U0126, SP600125, SB202190 and DDI-1 related compounds in dimethyl sulfoxide (DMSO). All of these stock solutions were stored at -80°C. Prior to use, small aliquots of each stock solution were thawed at room temperature and diluted with 1 x sperm medium (1 x SM, 50 mM Hepes-NaOH, pH 7.4, containing 45 mM NaCl, 5 mM

KCl, 1 mM $MgSO_4$, 5 mM $CaCl_2$ and 10 mM glucose) to prepare working solutions (Nishimura et al., 2015).

1-4-3 In vitro spermiogenesis assay

All steps were carried out at room temperature (~22°C). Spermatids were released by dissection of five males in 10 µl of Inhibitor Solution (1 x SM containing 1% DMSO or 100 µM of an inhibitor such as a MAPK inhibitor or a DDI-1-related compound). After 5-min incubation, 10 µl of SAF Solution (1 x SM containing 400 µg/ml Pron, 400 µg/ml ProK or 6 mM $ZnCl_2$) was added to the cells, and they were incubated for additional 15 min. For AEBSF-activation, males were dissected in 5 µl of Inhibitor Solution, and released spermatids were incubated for 5 min. The author next added 5 µl of 1 x SM containing 20 mM AEBSF, incubated this mixture for 3 more min and then added 10 µl of 1 x SM before a final 12-min incubation; the final volume of each preparation was 20 µl. To stain cellular membranes, 5 µl of FM1-43 Solution (1 x SM containing 20 µg/ml FM1-43) was added to the 20-µl preparation. Following a 5-min incubation, the fluorescently stained cells were observed under the LSM710 confocal microscope (Carl Zeiss), and DIC and fluorescent images were acquired.

1-4-4 Screening of compounds that block Pron-induced spermiogenesis

The Core Library was provided from the DDI (at the University of Tokyo, Japan). Out of ~9,600 entries that are contained in the library, the author screened 480 compounds for effects on an *in vitro* spermiogenesis assay (see the Section 1-4-3) using Pron and ProK as SAFs. Each candidate compound (10 mM

solutions in DMSO) was added to Inhibitor Solution (100 μM final), and its effect on spermatid activation was evaluated.

1-4-5 Synthesis of DDI-1 and its derivatives

The author discovered DDI-1 by screening of the Core Library that was provided by the DDI, Japan (www.ddi.u-tokyo.ac.jp). In this study, DDI-1 and three DDI-1 derivatives were synthesized for use in subsequent experiments. Below are strategies to synthesize those compounds.

1-4-5-1 DDI-1 (N-(2-(methyl(4-(methylthio)benzyl)amino)-2-oxoethyl)-4-phenoxybenzamide)

First, the author synthesized an intermediate compound 1 (INC1, 2-amino-N-methyl-N-(4-(methylthio)benzyl)acetamide). Dichloromethane was added to a mixture of N-methyl-1-(4-(methylthio)phenyl)methanamine, 1-hydroxybenzotriazole, N,N-diisopropylethylamine, 1-(3-dimethylaminopropyl)-3-ethylcarbodiimide hydrochloride and butoxycarbonyl-Gly-OH. The mixture was stirred for 15 min while being irradiated by microwaves at 120ºC. The reaction was quenched with 2 M HCl, followed by extraction of the aqueous layer with ethyl acetate. The combined organic layer was washed with saturated aqueous $NaHCO_3$ and brine, and then dried over $MgSO_4$. After filtration, the organic solvent was evaporated under reduced pressure. To the crude material, trifluoroacetic acid and CH_2Cl_2 was added and stirred for 6 h. After the reaction was completed, the pH of the solution was adjusted to 10 using 2 M NaOH, and the aqueous layer was extracted with chloroform. The combined organic layer

was dried over $MgSO_4$ and evaporated under the reduced pressure. The crude compound was purified by silica-gel flash column chromatography (ethyl acetate : hexane = 3 : 2).

As a next step, CH_2Cl_2 was added to a mixture containing the INC1, 4-phenoxy benzoic acid, 1-hydroxybenzotriazole and 1-(3-dimethylaminopropyl)-3-ethylcarbodiimide hydrochloride, and the whole mixture was stirred for 15 min while being irradiated by microwaves at 120ºC. Later steps were the same as those described above. The sample that had been purified by the silica-gel column chromatography was recrystallized out of a solvent mixture of ethyl acetate and hexane (3 : 2), and the yield of DDI-1 was 85%. This material was analyzed by mass spectrometry and ^{1}H-NMR (400 MHz) to confirm that the material we synthesized was identical to what was recovered from the DDI Core Library.

1-4-5-2 DDI-1A (4-(4-methoxyphenoxy)-N-(2-(methyl(4-(methylthio)benzyl) amino)-2-oxoethyl)benzamide)

Dichloromethane was added to a mixture of the INC1, 4-(4-methoxyphenoxy)benzoic acid, 1-hydroxybenzotriazole and 1-(3-dimethylaminopropyl)-3-ethylcarbodiimide hydrochloride, and the whole mixture was stirred for 15 min while being irradiated by microwaves at 120ºC. Later steps were the same as those for the synthesis of DDI-1, and the yield of DDI-1A was 81%.

1-4-5-3 DDI-1C (4-(4-fluorophenoxy)-N-(2-(methyl(4-(methylthio)benzyl) amino)-2-oxoethyl)benzamide)

Dichloromethane was added to a mixture of the INC1, 4-(4-fluorophenoxy)benzoic acid, 1-hydroxybenzotriazole and 1-(3-dimethylaminopropyl)-3-ethylcarbodiimide hydrochloride, and the whole mixture was stirred for 15 min while being irradiated by microwaves at 120ºC. Later steps were the same as those for the synthesis of DDI-1, and the yield of DDI-1C was 58%.

1-4-5-4 DDI-1H (N-methyl-N-(4-methylsulfanyl-benzyl)-4-oxo-4-(4-phenoxy phenyl)-butyramide)

Dichloromethane was added to a mixture of N-methyl-1-(4-(methylthio)phenyl)methanamine, 4-oxo-4-(4-phenoxyphenyl)butanoic acid, 1-hydroxybenzotriazole and 1-(3-dimethylaminopropyl)-3-ethylcarbodiimide hydrochloride, and the whole mixture was stirred for 20 min while being irradiated by microwaves at 120ºC. Later steps were the same as those for the synthesis of DDI-1, and the yield of DDI-1H was 40%.

1-4-6 Forward genetic screening of mutant worms of which spermatids are resistant to DDI-1

C. elegans hermaphrodites were mutagenized with EMS according to standard methods (Brenner, 1974). *him-8(tm611)* hermaphrodites, which produce ~40% males, were used to easily obtain males among self-progeny. Briefly, *him-8(tm611)* worms at the fourth larval (L4) stage (P_0, ~60% of total were hermaphrodites) were incubated with 50 mM EMS at room temperature for ~4 h. Ten mutagenized P_0 worms were transferred onto a single 60-mm nematode

growth medium (NGM) agar plate containing *E. coli* OP50 lawns (20 plates, 200 P_0 worms total). After ~100 fertilized F_1 eggs were laid onto each plate, the P_0 worms were removed and discarded. Twenty-five F_1 hermaphrodites were picked from each plate and individually transferred onto NGM plates (500 F_1 worms total). We picked ~20 F_2 males from each plate, and they were individually examined by our *in vitro* spermiogenesis assay (see the Section 1-4-3) using Pron and DDI-1 to identify DDI-1 resistant males. If a tested F_2 male was positive in the assay, the author repeated this process on successive males in his pedigree until hermaphrodites were identified that produced 100% DDI-1 resistant sons. Such hermaphrodites were outcrossed with N2 males five times, in order to remove unrelated mutations as much as possible.

References

Andrusiak, M. G., & Jin, Y. (2016). Context specificity of stress-activated mitogen-activated protein (MAP) kinase signaling: the story as told by Caenorhabditis elegans. *Journal of Biological Chemistry*, *291*(15), 7796-7804. https://doi: 10.1074/jbc.R115.711101

Arduengo, P. M., Appleberry, O. K., Chuang, P., & L'Hernault, S. W. (1998). The presenilin protein family member SPE-4 localizes to an ER/Golgi derived organelle and is required for proper cytoplasmic partitioning during Caenorhabditis elegans spermatogenesis. *Journal of Cell Science*, *111*(Pt 24), 3645-3654.

Baldi, C., Cho, S., & Ellis, R. E. (2009). Mutations in two independent pathways are sufficient to create hermaphroditic nematodes. *Science*, *326*(5955), 1002-1005. doi: 10.1126/science.1176013

Brenner, S. (1974). The genetics of Caenorhabditis elegans. *Genetics*, *77*(1), 71-94.

Ellis, R. E., & Stanfield, G. M. (2014). The regulation of spermatogenesis and sperm function in nematodes. *Seminars in Cell & Developmental Biology*, *29*, 17-30. doi: 10.1016/j.semcdb.2014.04.005

Fenker, K. E., Hansen, A. A., Chong, C. A., Jud, M. C., Duffy, B. A., Norton, J. P., Hansen, J. M., & Stanfield, G. M. (2014). SLC6 family transporter SNF-10 is required for protease-mediated activation of sperm motility in C. elegans. *Developmental Biology*, *393*(1), 171-182. https://doi: 10.1016/j.ydbio.2014.06.001

Florman, H. M., & Fissore, R. A. (2015). Fertilization in mammals. *Knobil and Neill's Physiology of Reproduction* (4th ed.), Cambridge, MA: Academic Press, 149-196. https://doi.org/10.1016/B978-0-12-397175-3.00004-1

Geldziler, B., Chatterjee, I., & Singson, A. (2005). The genetic and molecular analysis of spe-19, a gene required for sperm activation in Caenorhabditis elegans. *Developmental Biology*, *283*(2), 424-436.

Gleason, E. J., Hartley, P. D., Henderson, M., Hill-Harfe, K. L., Price, P. W., Weimer, R. M., Kroft, T. L., Zhu, G. D., Cordovado, S., & L'Hernault, S. W. (2012). Developmental genetics of secretory vesicle acidification during Caenorhabditis elegans spermatogenesis. *Genetics*, *191*(2), 477-491. doi: 10.1534/genetics.112.139618

Gosney, R., Liau, W. S., & Lamunyon, C. W. (2008). A novel function for the presenilin family member spe-4: inhibition of spermatid activation in Caenorhabditis elegans. *BMC Developmental Biology*, *8*, 44. https://doi: 10.1186/1471-213X-8-44

Inoue, N., & Wada, I. (2018). Monitoring dimeric status of IZUMO1 during the acrosome reaction in living spermatozoon. *Cell Cycle*, *17*(11), 1279-1285. doi: 10.1080/15384101.2018.1489181

Krauchunas, A. R., Mendez, E., Ni, J. Z., Druzhinina, M., Mulia, A., Parry, J., Gu, S. G., Stanfield, G. M., & Singson, A. (2018). spe-43 is required for sperm activation in C. elegans. *Developmental Biology*, *436*(2), 75-83. https://doi: 10.1016/j.ydbio.2018.02.013

Li, M. W., Mruk, D. D., & Cheng, C. Y. (2009). Mitogen-activated protein kinases in male reproductive function. *Trends in Molecular Medicine*, *15*(4), 159-168.

https://doi: 10.1016/j.molmed.2009.02.002

Liau, W. S., Nasri, U., Elmatari, D., Rothman, J., & LaMunyon, C. W. (2013). Premature sperm activation and defective spermatogenesis caused by loss of spe-46 function in Caenorhabditis elegans. *PLoS One*, *8*(3), e57266. https://doi: 10.1371/journal.pone.0057266

L'Hernault, S. W., Shakes, D. C., & Ward, S. (1988). Developmental genetics of chromosome I spermatogenesis-defective mutants in the nematode Caenorhabditis elegans. *Genetics*, *120*(2), 435-452.

L'Hernault, S. W., & Arduengo, P. M. (1992). Mutation of a putative sperm membrane protein in Caenorhabditis elegans prevents sperm differentiation but not its associated meiotic divisions. *Journal of Cell Biology*, *119*(1), 55-68.

L'Hernault, S. W. (2009). The genetics and cell biology of spermatogenesis in the nematode C. elegans. *Molecular and Cellular Endocrinology*, *306*(1-2), 59-65. https://doi: 10.1016/j.mce.2009.01.008

Liu, Z., Chen, L., Shang, Y., Huang, P., & Miao, L. (2013). The micronutrient element zinc modulates sperm activation through the SPE-8 pathway in Caenorhabditis elegans. *Development*, *140*(10), 2103-2107. https://doi: 10.1242/dev.091025

Liu, Z., Wang, B., He, R., Zhao, Y., & Miao, L. (2014). Calcium signaling and the MAPK cascade are required for sperm activation in Caenorhabditis elegans. *Biochimica et Biophysica Acta*, *1843*(2), 299-308. https://doi: 10.1016/j.bbamcr.2013.11.001

Ma, X., Zhao, Y., Sun, W., Shimabukuro, K., & Miao, L. (2012). Transformation: How do nematode sperm become activated and crawl? *Protein Cell*, *3*(10),

755-761. https://doi: 10.1007/s13238-012-2936-2

Minniti, A. N., Sadler, C., & Ward, S. (1996). Genetic and molecular analysis of spe-27, a gene required for spermiogenesis in Caenorhabditis elegans hermaphroditesGenetics. *Genetics*, *143*(1), 213-223.

Muhlrad, P. J., & Ward, S. (2002). Spermiogenesis initiation in Caenorhabditis elegans involves a casein kinase 1 encoded by the spe-6 gene. *Genetics*, *161*(1), 143-155.

Muhlrad, P. J., Clark, J. N., Nasri, U., Sullivan, N. G., & LaMunyon, C. W. (2014). SPE-8, a protein-tyrosine kinase, localizes to the spermatid cell membrane through interaction with other members of the SPE-8 group spermatid activation signaling pathway in C. elegans. *BMC Genetics*, *15*, 83. https://doi: 10.1186/1471-2156-15-83

Nance, J., Minniti, A. N., Sadler, C., & Ward, S. (1999). spe-12 encodes a sperm cell surface protein that promotes spermiogenesis in Caenorhabditis elegans. *Genetics*, *152*(1), 209-220.

Nance, J., Davis, E. B., & Ward, S. (2000). spe-29 encodes a small predicted membrane protein required for the initiation of sperm activation in Caenorhabditis elegans. *Genetics*, *156*(4), 1623-1633.

Nelson, G. A., & Ward, S. (1980). Vesicle fusion, pseudopod extension and amoeboid motility are induced in nematode spermatids by the ionophore monensin. *Cell*, *19*(2), 457-464.

Nishimura, H., & L'Hernault, S. W. (2010). Spermatogenesis-defective (spe) mutants of the nematode Caenorhabditis elegans provide clues to solve the puzzle of male germline functions during reproduction. *Developmental*

Dynamics, *239*(5), 1502-1514. https://doi: 10.1002/dvdy.22271

Nishimura, H., Tajima, T., Comstra, H. S., Gleason, E. J., & L'Hernault, S. W. (2015). The immunoglobulin-like gene spe-45 acts during fertilization in Caenorhabditis elegans like the mouse Izumo1 gene. *Current Biology*, *25*(24), 3225-3231. https://doi: 10.1016/j.cub.2015.10.056

Nishimura, H., & L'Hernault, S. W. (2017). Spermatogenesis. *Current Biology*, *27*(18), R988-R994. https://doi: 10.1016/j.cub.2017.07.067

Reinke, V., Smith, H. E., Nance, J., Wang, J., Van Doren, C., Begley, R., Jones, S. J., Davis, E. B., Scherer, S., Ward, S., & and Kim, S. K. (2000). A global profile of germline gene expression in C. elegans. *Molecular Cell*, *6*(3), 605-616.

Reinke, V., Gil, I. S., Ward, S., & Kazmer, K. (2004). Genome-wide germline-enriched and sex-biased expression profiles in Caenorhabditis elegans. *Development*, *131*(2), 311-323.

Roux, P. P., & Blenis, J. (2004). ERK and p38 MAPK-activated protein kinases: a family of protein kinases with diverse biological functions. *Microbiology and Molecular Biology Reviews*, *68*(2), 320-344.

Shakes, D. C., & Ward, S. (1989). Initiation of spermiogenesis in C. elegans: a pharmacological and genetic analysis. *Developmental Biology*, *134*(1), 189-200.

Smith, P., Leung-Chiu, W. M., Montgomery, R., Orsborn, A., Kuznicki, K., Gressman-Coberly, E., Mutapcic, L., & Bennett, K. (2002). The GLH proteins, Caenorhabditis elegans P granule components, associate with CSN-5 and

KGB-1, proteins necessary for fertility, and with ZYX-1, a predicted cytoskeletal protein. *Developmental Biology*, *251*(2), 333-347.

Smith, J. R., & Stanfield, G. M. (2011). TRY-5 is a sperm-activating protease in Caenorhabditis elegans seminal fluid. *PLoS Genetics*, *7*(11), e1002375. https://doi: 10.1371/journal.pgen.1002375

Stanfield, G. M., & Villeneuve, A. M. (2006). Regulation of sperm activation by SWM-1 is required for reproductive success of C. elegans males. *Current Biology*, *16*(3), 252-263.

Stival, C., Puga Molina Ldel, C., Paudel, B., Buffone, M. G., Visconti, P. E., & Krapf, D. (2016). Sperm capacitation and acrosome reaction in mammalian sperm. *Advances in Anatomy, Embryology, and Cell Biology*, *220*, 93-106. doi: 10.1007/978-3-319-30567-7_5

Takayama, J., & Onami, S. (2016). The sperm TRP-3 channel mediates the onset of a Ca^{2+} wave in the fertilized C. elegans oocyte. *Cell Reports*, *15*(3), 625-637. doi: 10.1016/j.celrep.2016.03.040

Toshimori, K., Tanii, I., Araki, S., & Oura, C. (1992). Characterization of the antigen recognized by a monoclonal antibody MN9: unique transport pathway to the equatorial segment of sperm head during spermiogenesis. *Cell and Tissue Research*, *270*(3), 459-468.

Varkey, J. P., Jansma, P. L., Minniti, A. N., & Ward, S. (1993). The Caenorhabditis elegans spe-6 gene is required for major sperm protein assembly and shows second site non-complementation with an unlinked deficiency. *Genetics*, *133*(1), 79-86.

Ward, S., Hogan, E., & Nelson, G. A. (1983). The initiation of spermiogenesis in the nematode Caenorhabditis elegans. *Developmental Biolology*, *98*(1), 70-79.

Washington, N. L., & Ward, S. (2006). FER-1 regulates Ca2+-mediated membrane fusion during C. elegans spermatogenesis. *Journal of Cell Science*, *119*(Pt 12), 2552-2562. doi: 10.1242/jcs.02980

Wei, Q., Zhao, Y., Guo, Y., Stomel, J., Stires, R., & Ellis, R. E. (2014). Co-option of alternate sperm activation programs in the evolution of self-fertile nematodes. *Nature Communication*, *5*, 5888. doi: 10.1038/ncomms6888

Wijayanti, N., Kietzmann, T., & Immenschuh, S. (2005). Heme oxygenase-1 gene activation by the NAD(P)H oxidase inhibitor 4-(2-aminoethyl) benzenesulfonyl fluoride via a protein kinase B, p38-dependent signaling pathway in monocytes. *Journal of Biological Chemistry*, *280*(23), 21820-21829.

Zannoni, S., L'Hernault, S. W., & Singson, A. W. (2003). Dynamic localization of SPE-9 in sperm: a protein required for sperm-oocyte interactions in Caenorhabditis elegans. *BMC Developmental Biology*, *3*, 10.

Zhao, Y., Tan, C. H., Krauchunas, A., Scharf, A., Dietrich, N., Warnhoff, K., Yuan, Z., Druzhinina, M., Gu, S. G., Miao, L., Singson, A., Ellis, R. E., & Kornfeld, K. (2018). The zinc transporter ZIPT-7.1 regulates sperm activation in nematodes. *PLoS Biology*, *16*(6), e2005069. https://doi: 10.1371/journal.pbio.2005069

Xu, X. Z., & Sternberg, P. W. (2003). A C. elegans sperm TRP protein required for sperm-egg interactions during fertilization. *Cell*, *114*(3), 285-297.

PART 2

Functional analysis of *spe-45* as a member of the *spe-9* class genes, essentially required during *C. elegans* gamete fusion

Abstract

The *Caenorhabditis elegans spe-9* class genes, which are predominantly or specifically expressed in the male germline, play indispensable roles during fertilization. The mouse *Izumo1* gene encodes a sperm transmembrane (TM) protein with a single immunoglobulin (Ig)-like domain that is essential for gamete fusion *via* binding to the oocyte-surface protein JUNO. Nishimura *et al.* (2015) hypothesized that *C. elegans* has a new member of the *spe-9* class coding for an IZUMO1-like protein. By a reverse genetic analysis, they identified *F28D1.8*, a male germline-enriched gene encoding a TM protein with a single Ig-like domain. Since *F28D1.8* mutant hermaphrodites were self-sterile but became fertile as being mated with wild-type males, a function(s) of the gene was likely confined to the male germline. Thereby, *F28D1.8* was renamed *spe-45*. *spe-45* mutant worms normally underwent spermatogenesis (spermatid production *via* meiosis) and spermiogenesis (spermatid activation into actively motile spermatozoa). These data imply that *spe-45* might be involved in a later event(s) of male germline functions such as fertilization. In this study, the author examined whether *spe-45* is a novel member of the *spe-9* class. It was suggested that *spe-45* mutant spermatozoa have a defect in gamete fusion by counting the number of self-sperm in the spermatheca of *spe-45* mutant worms. Moreover, *spe-45* mutant worms were rescued by a transgene expressing chimeric SPE-45 protein where its Ig-like domain was replaced by the Ig-like domain of mouse IZUMO1. Hence, *C. elegans* SPE-45 and mouse IZUMO1 appear to have retained a common function(s) that is required during fertilization.

Since the folate receptor-like protein JUNO is an essential *trans*-partner of IZUMO1, the author also examined whether or not the *C. elegans folt-2* and *folt-3* genes, encoding folate transporters with unknown functions, are involved in fertilization. Hermaphrodites carrying mutations in either *folt-2* or *folt-3* were indistinguishable from wild-type worms in self-fertility, suggesting that *folt-2* and *folt-3* genes are not essential for gamete fusion unlike *spe-45* gene.

2-1 Introduction

Fertilization is a pivotal process of sexual reproduction in eukaryotes. In the mouse, fertilization consists of multiple interactions of spermatozoa with the cumulus cell layer (CL), the zona pellucida (ZP) and the oocyte plasma membrane (PM) (Figure 2.1, left) (Florman & Fissore, 2015). The proteins that have been thought to be important for these interactions evolve rapidly, likely in order to prevent the production of cross-species hybrids (Swanson & Vacquier, 2002; Wyckoff et al., 2007; Haerty et al., 2007). The basic local alignment search tool (BLAST) is commonly used to identify orthologs of target genes. However, perhaps this way is challenging if the targets are required for gamete interactions during fertilization.

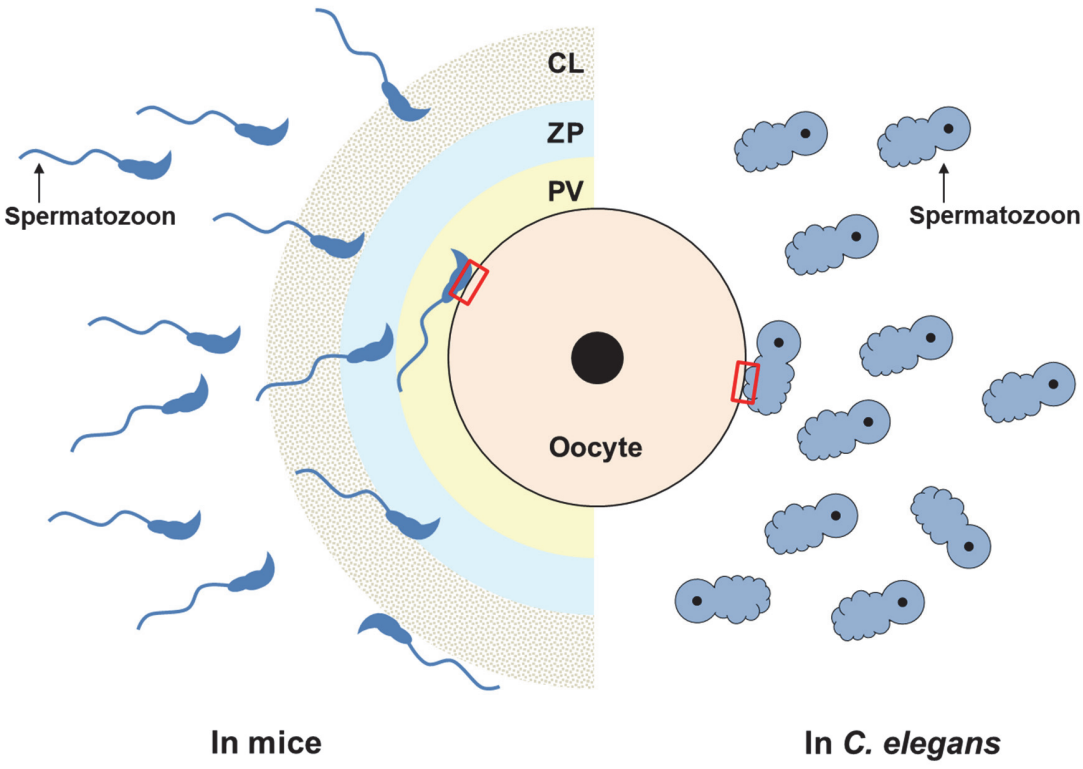

Figure 2.1 Schematic comparison of fertilization in the mouse and *C. elegans*. (Left) In the mouse, a spermatozoon must pass through the CL and the ZP for entry into the perivilelline space (PV), where the oocyte PM is exposed. The spermatozoon becomes acrosome-reacted prior to contacting with the ZP, and gamete fusion occurs on the equatorial segment of the acrosome-reacted sperm (shown by a red square). (Right) Since a *C. elegans* oocyte lacks any types of accessory cells and thick egg coats such as the CL and the ZP, respectively, a spermatozoon directly binds to and fuses with the oocyte PM through the pseudopod (shown by a red square). This figure was prepared on the basis of the review by Nishimura & L'Hernault (2016).

Caenorhabditis elegans has several advantages as a model organism for studying sperm-oocyte fusion. For instance, a *C. elegans* oocyte lacks accessory cells and a thick egg coat, unlike mammalian oocytes (Figure 2.1, right), so that the fusogenic reaction in *C. elegans* can be examined more simply than those in mammals. Moreover, *C. elegans* genes have a category called "the *spe-9* class" (Nishimura & L'Hernault, 2010; Marcello et al., 2013). Its members essentially act during fertilization (in other words, "during gamete fusion"), while such genes are dispensable during spermatogenesis to produce spermatids *via* meiosis and during spermiogenesis to activate spermatids into motile amoeboid spermatozoa. Five *spe-9* class genes have been so far identified (*spe-9* (Singson et al., 1998; Zannoni et al., 2003; Putiri et al., 2004), *spe-38* (Chatterjee et al., 2005; Singaravelu et al., 2015), *spe-41*/*trp-3* (Xu & Stenberg, 2003; Takayama & Onami, 2016), *spe-42* (Kroft et al., 2005) and *spe-49* (Wilson et al., 2017)), and they all exhibit predominant or specific expression in the *C. elegans* male germline. Human and/or mouse orthologs of those genes can be predicted according to the domain architectures of each SPE-9

class protein (Table 2.1), but it is unknown whether or not the mammalian orthologs are functionally related to the *C. elegans spe-9* class genes.

Table 2.1 *C. elegans spe-9* class genes involved during fertilization

Gene	LG[1]	TM[2]	Domain/Feature	Localization[3]	Predicted ortholog[4]
spe-9	I	1	10 EGF-like domains (651 aa)	PM of spermatid Pseudopod of sperm	*DLL1*, *DLL3*, *DLL4* (h)
spe-38	I	4	No clear domain (179 aa)	MOs of spermatid Pseudopod of sperm	Not found in mammals
spe-41/ trp-3	III	6	TRPC family (854 aa)	MOs of spermatid PM of sperm	*TRPC6* (h), *Trpc6* (m)
spe-42	V	6	DC-STAMP and RING-finger domains (774 aa)	ND	*DCST2* (h), *Dcst1* (m)
spe-49	V	6	DC-STAMP and RING-finger domains (772 aa)	ND	*DCST2* (h), *Dcst1* (m)

[1]Abbreviations: LG, linkage group; TM, transmembrane; EGF, epidermal growth factor; aa, amino acid; MO, membranous organelle; TRPC, transient receptor potential-canonical; DC-STAMP, dendritic cell-specific transmembrane protein; ND, not determined.
[2]The number of TM domain in each predicted protein.
[3]PM indicates the entire cell surface in this table.
[4]Human (h) and/or mouse (m) orthologous genes were predicted by WormBase (www.wormbase.org) on the basis of their nucleotide and/or predicted protein sequences.

On the other hand, studies using knockout mice showed that *Izumo1* (Inoue et al., 2005) and *Spaca6* (Lorenzetti et al., 2014) genes, encoding sperm-specific transmembrane (TM) proteins carrying a single immunoglobulin (Ig)-like domain, are indispensable for spermatozoa to fuse with the oocyte PM. During the sperm acrosome reaction, which is well known to be prerequisite for gamete fusion, IZUMO1 relocates onto the surface of the equatorial segment of sperm heads, where spermatozoa bind to and fuse with the oocyte PM. Then, IZUMO1 becomes capable of binding to JUNO on the oocyte surface, which is a glycosylphosphatidylinositol (GPI)-anchored folate receptor-like protein (Bianchi et al., 2014).

Nishimura *et al.* (2015) hypothesized that the *C. elegans spe-9* class has a new member encoding an IZUMO1/SPACA6-like protein. By reverse (Nishimura et al., 2015) and forward (Singaravelu et al., 2015) genetic approaches, the *C. elegans* gene *F28D1.8* was identified. This gene is ~2.4 kbp in length and composed of eight exons on *C. elegans* chromosome IV (Figure 2.2A). The *tm3715* allele deletes 418-bp nucleotides from the *F28D1.8* sequence (Figure 2.2A). The predicted F28D1.8 protein of 492 amino acids (aa) contains a hydrophobic region and acidic and basic amino acid clusters, as well as one Ig-like and one TM domains (Figure 2.2B). *tm3715* deletes a part of *F28D1.8* that encodes the TM and the cytoplasmic tail domains, likely resulting in a non-functional or absent protein.

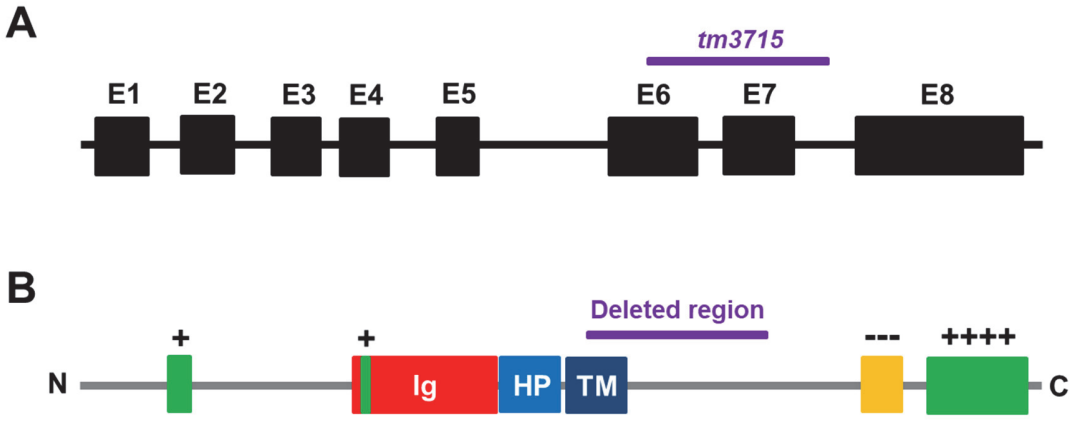

Figure 2.2 Genomic and predicted protein structures of *C. elegans F28D1.8*. (A) The genomic structure of *F28D1.8*. *F28D1.8* is a ~2.4-kbp gene consisting of eight exons (E1-E8). A purple, thick bar shows the area deleted in the *tm3715* allele. (B) The predicted protein structure of *F28D1.8*. The SOSUI program predicts a hydrophobic region (HP) outside of the TM domain (http://harrier.nagahama-i-bio.ac.jp/sosui/). The deduced amino acid sequence also contains positively (+) and negatively (-) charged regions, and numbers of the "+" and "-" symbols represent relative numbers of basic and acidic residues,

respectively. This figure was prepared on the basis of the report by Nishimura *et al*. (2015).

F28D1.8(tm3715) hermaphrodites were self-sterile but became fertile as being outcrossed with wild-type males, demonstrating that the functional role(s) of *F28D1.8* is confined to the male germline (Nishimura et al., 2015; Singaravelu et al., 2015). Thereby, *F28D1.8* was renamed *spe-45*; *spe* genes are defined to act in male germline functions. Moreover, *spe-45(tm3715)* males produced spermatids that were indistinguishable from wild-type spermatids in number and cytology, indicating that spermatogenesis (production of spermatids *via* meiosis) is normal (Nishimura et al., 2015). The mutant spermatids could be activated into spermatozoa *in vitro* by the bacterial protease mixture Pronase (Nishimura et al., 2015). After *spe-45(tm3715)* males mated with *fem-1(hc17)* hermaphrodites, which are substantially females because of no self-sperm (Nelson et al., 1078), numerous spermatozoa were observed in the spermatheca of the females, suggesting that spermatids ejaculated from the *spe-45* mutant males activated into spermatozoa in the uterus and then crawled into the spermatheca of the *fem-1* mutant females (Nishimura et al., 2015). These data likely show that *spe-45(tm3715)* worms normally undergo spermiogenesis (activation of spermatids into spermatozoa). Therefore, among *C. elegans* male germline functions, *spe-45* seemed to be dispensable during spermatogenesis and spermiogenesis.

In this study, the author examined whether or not *spe-45* acts during *C. elegans* fertilization (fusion of spermatozoa with oocytes). Since the number of self-sperm in the spermatheca of *spe-45(tm3715)* worms was not reduced unlike

wild type (see Figure 2.3), perhaps fertilization did not occur. This result seems to show that *spe-45* belongs to the *spe-9* class. When a transgene encoding SPE-45 protein in which the native Ig-like domain was replaced by that of mouse IZUMO1 was expressed in *spe-45(tm3715)* worms, the self-sterility of the mutant hermaphrodites were rescued. Therefore, the Ig-like domains of SPE-45 and IZUMO1 might possess a common role(s) during gamete fusion. Moreover, to explore a possibility that a folate-related protein on the surface of *C. elegans* oocytes might be a SPE-45 receptor, the author created *C. elegans* mutant lines in which either *folt-2* or *folt-3* genes were mutated, encoding folate transporter proteins with unknown functions. These two mutants were normal in self-fertility, suggesting that the functional roles of *folt-2* and *folt-3* are dispensable during fertilization.

2-2 Results

2-2-1 spe-45 mutant spermatozoa cannot fertilize oocytes in the spermatheca

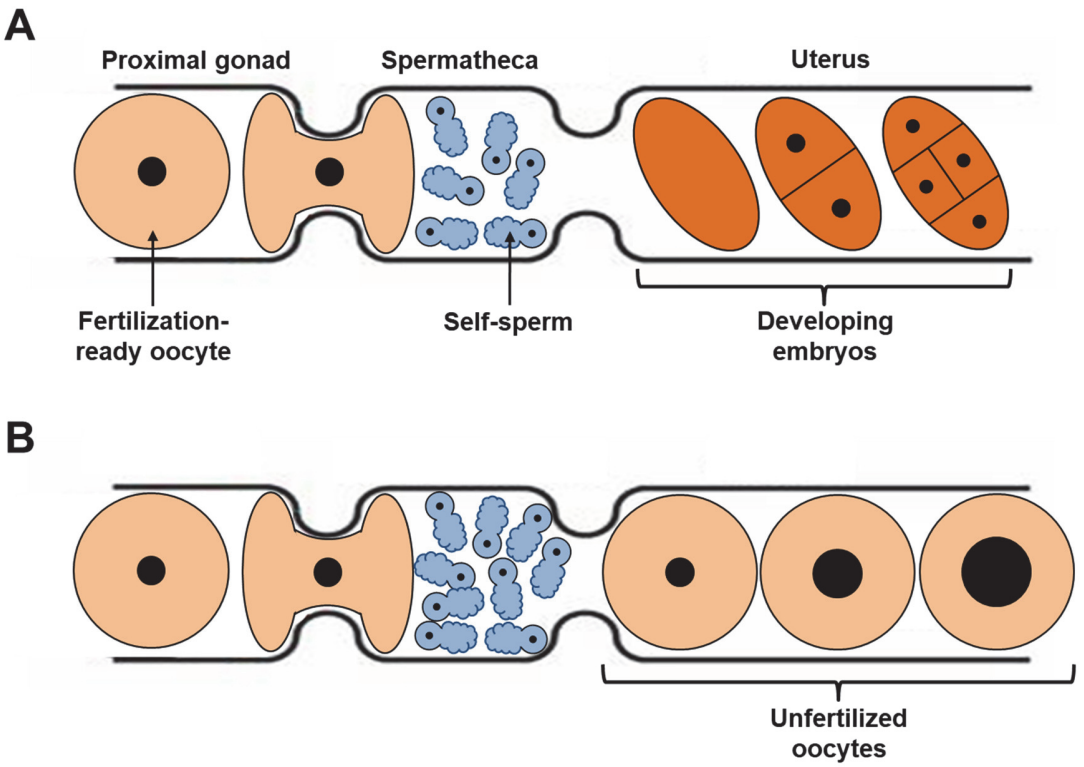

Figure 2.3 Fertilization does not occur in *spe-9* class mutants. This figure shows how ovulation, fertilization and early embryogenesis occur in the gonad of wild-type (A) and *spe-9* class mutant (B) hermaphrodites. (A) Following ovulation of a fertilization-competent oocyte into the spermatheca, a hermaphrodite-derived spermatozoon (self-sperm) fertilizes that oocyte. Then, the fertilized oocyte moves into the uterus, begins embryogenesis and is laid through the vulva. A wild-type hermaphrodite only lays unfertilized oocytes after it has completely used up all spermatozoa. As a sperm-released factor, called the major sperm protein (MSP) (Miller et al., 2001), stimulates ongoing ovulation, the hermaphrodite that is close to the end of her lifespan will always lays low numbers of unfertilized oocytes. (B) When any of the *spe-9* class genes are mutated, mutant self-sperm are normal in number, motility and cytology. However, the spermatozoa cannot fertilize oocytes in the

spermatheca. Despite being fertilization-defective, *spe-9* class mutant sperm are competent to stimulate ovulation, so that mutant hermaphrodites lay larger numbers of unfertilized oocytes than wild type as young adults. After migration into the uterus, the unfertilized oocyte undergoes endomitotic DNA replication without cell division and is subsequently laid onto the worm growth plate. If a *spe-9* class mutant male inseminates a wild-type hermaphrodite, mutant male-derived spermatozoa can outcompete hermaphrodite-derived spermatozoa in the spermatheca, but they are incapable of fertilizing oocytes. This figure was prepared on the basis of the report by Nishimura *et al*. (2015).

As shown in Figure 2.3, ~300 wild-type self-sperm are all consumed by fertilization that occurs in the spermatheca (Ward & Carrel et al., 1979). For this study, hermaphrodites at the fourth larval (L4) stage were incubated at 20ºC for either 24 or 72 h. Then, those worms were fixed and 4',6-diamidino-2-phenylindole (DAPI)-stained to visualize countable self-sperm (Figure 2.4,Table 2.2). In each spermatheca of wild-type N2 hermaphrodites, there were ~140 self-sperm at 24 h post the L4 stage (Figure 2.4A,A',Table 2.2), but their numbers were reduced to almost zero at 72 h (Figure 2.4E,E',Table 2.2). Similar data were also obtained in *him-5(e1490)* hermaphrodites (unpublished results). In the known "*spe-9* class" mutants *spe-9(eb19)* (Singson et al., 1998) and *spe-42(tm2421)* (Kroft et al., 2005) and also in *spe-45(tm3715)* worms, like wild type, there were numerous self-sperm in each spermatheca at 24 h (~90 *spe-9* sperm (Figure 2.4B,B',Table 2.2), ~220 *spe-42* sperm (Figure 2.4C,C',Table 2.2) and ~180 *spe-45* sperm (Figure 2.4D,D',Table 2.2). However, unlike wild type, many self-sperm still resided in the spermathecae of *spe-9* (~50 sperm), *spe-42* (~220 sperm) and *spe-45* (~110 sperm) mutant hermaphrodites even at 72 h (Figure 2.4F-H,F'-H',Table 2.2). Intriguingly, numbers of *spe-9* and *spe-45* self-

sperm at 72 h were reduced to 52 and 63%, respectively, of those at 24 h, while numbers of *spe-42* self-sperm at 24 h were similar to those at 72 h. Such reduction of *spe-9* self-sperm was also observed previously in hermaphrodites bearing different mutant alleles (L'Hernault et al., 1988).

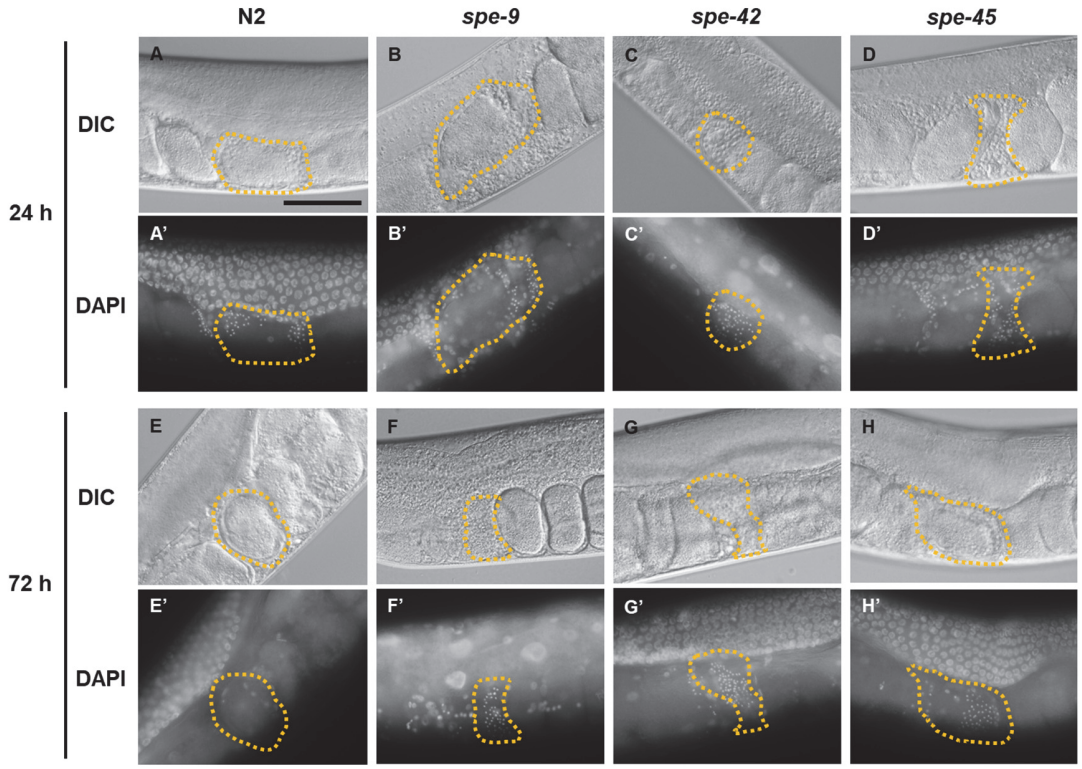

Figure 2.4 Self-fertilization is not observed in *spe-45* mutant worms. At 24 and 72 h after the L4 stage, N2 (A,A',E,E'), *spe-9(eb19); him-5(e1490)* (B,B',F,F'), *spe-42(tm2421)* (C,C',G,G') and *spe-45(tm3751)* (D,D',H,H') hermaphrodites were fixed, treated with DAPI to stain self-sperm nuclei, and then observed to check if self-sperm numbers are reduced due to participation in fertilization. Orange broken lines highlight the position of the spermatheca. DIC, differential interference contrast microscopy. A scale bar of 50 μm shown in panel (A) applies to all of the images in this figure. See also Table 2.2 that summarizes the number of self-sperm in each spermatheca of tested worm strains. This figure was prepared on the basis of the report by Nishimura *et al*. (2015).

Table 2.2 Number of self-sperm after repeated ovulation

Genotype	Period post L4 stage	
	24 h	72 h
N2	139 ± 33 (16)	2 ± 4 (18)
spe-9(eb19)	93 ± 30 (23)	48 ± 30 (18)
spe-42(tm2421)	217 ± 29 (22)	218 ± 36 (20)
spe-45(tm3715)	175 ± 20 (18)	110 ± 18 (18)

Hermaphrodites at the L4 stage were incubated at 20ºC for 24 or 72 h, fixed and stained with DAPI to fluorescently visualize sperm nuclei, which were counted to determine the number of hermaphrodite-derived spermatozoa. The data show that many self-sperm are present in each spermatheca and are indicated as mean ± SEM (n). Note that the mean numbers of self-sperm are for one spermatheca and each hermaphrodite has two spermathecae, so that the total number of sperm per hermaphrodite is approximately twice the mean numbers shown above. This table, prepared on the basis of the report by Nishimura *et al.* (2015), is related to Figure 2.4. SEM, standard error of the mean.

One of the possible interpretations for these results is that, in *spe-9* and *spe-45* mutants, self-sperm can bind to the oocyte PM, but they cannot complete gamete fusion. Oocytes that failed to be fertilized in the spermatheca, on which a fraction of self-sperm are still binding, move into the uterus, undergo endomitotic DNA replication without cell division, and are eventually excluded with self-sperm from the worm body through the vulva. In *spe-42* mutant hermaphrodites, self-sperm are presumably incapable of binding to the oocyte PM, so that self-sperm keep to stay in the spermatheca. It is worth noting that mouse spermatozoa lacking IZUMO1 can bind to, but not fuse with, the oocyte PM (Inoue et al., 2005; Inoue et al., 2013).

2-2-2 Ig-like domains of SPE-45 and IZUMO1 have a common function in fertilization

Since Ig-like domains have considerable sequence diversity but similar three-dimensional structures (Bork et al., 1994; Halaby et al., 1999), the author tested if the Ig-like domains of SPE-45 and IZUMO1 are functionally similar.

A

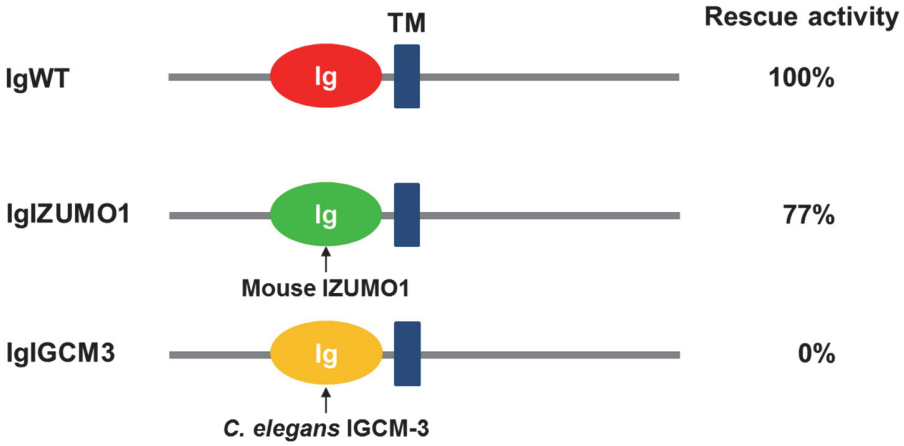

B

```
SPE-45 (C.elegans) :CDEM-NRKKKRK-----KHEEIEFVEWFVNGKRINP-SWFDWRVS
SPE-45 (C.briggsae):CDQE-NRKKNGK-----KKEEVEFVEWFVNGKRIDP-SWFDWRVS
SPE-45 (C.remanei) :CDEE-NRKRNRK-----KNEEIEFIEWFVNGKRIQP-SWFDWRVS
SPE-45 (C.brenneri):CDED-DRRNNRK-----KNAEVEFIEWFVNGRRITP-SWFDWRVS
IZUMO1 (Mouse)     :CEKQ-LHICRKSLDCGERHIEVHRSE------DLVLDCLLSWHRA
IZUMO1 (Human)     :CKKE-VHACRKSYDCGERNVEVPQME------DMILDCELNWHQA
IGCM-3 (C.elegans) :CEVEGNPRP------------IVY--WRM--RKPNGDVVDAACPQ

SPE-45 (C.elegans) :---VSIDGHLGIW------------------PI-GEGDGGHFEC
SPE-45 (C.briggsae):---VSIDGKLGVW------------------PI-GVDDSGHFEC
SPE-45 (C.remanei) :---VSMDGKLGIW------------------PI-GVGDSGHFEC
SPE-45 (C.brenneri):---VSSDGRLGIW------------------PI-GIDDSGQFEC
IZUMO1 (Mouse)     :SKGLTDYSFYRVWENSSETLIAKGKEPYLTKSMVGPEDAGNYRC
IZUMO1 (Human)     :SEGLTDYSFYRVWGNNTETLVSKGKEATLTKPMVGPEDAGSYRC
IGCM-3 (C.elegans) :GLEGQYQELPPEGGRSANIVRLTALCSLR---ISNYSYSGQYWC
```

Figure 2.5 Ig-like domains can be interchangeable between SPE-45 and IZUMO1. (A) Transgenes used for the rescue assay in this study. The author constructed three transgenes encoding SPE-45 protein in which the Ig-like domain was the one naturally found in SPE-45 (IgWT) or it was replaced by those of mouse IZUMO1 (IgIZUMO1) or *C. elegans* IGCM-3 (IgIGCM3). Non-transgenic *spe-45(tm3715)* hermaphrodites produced no F_1 progeny (n = 15) (data not shown). Normalizing for *spe-45* mutant worms expressing the IgWT transgene as having a relative brood size of self-progeny at 100.0 ± 15.0% levels (mean ± SEM, n = 12), the relative brood sizes of the same hermaphrodites expressing the IgIZUMO1 and IgIGCM3 transgenes were 76.8 ± 9.7% (n = 14) and 0% (n = 15), respectively.

(B) An alignment of Ig-like loops. The amino acid sequences of the Ig-like loop regions in *Caenorhabditis* SPE-45 orthologs, human and mouse IZUMO1s and *C. elegans* IGCM-3 were aligned. Red and green letters indicate identical and chemically similar residues, respectively, to those of *C. elegans* SPE-45. Blue letters indicate residues that are conserved in all of those proteins. The amino acid sequences of SPE-45 orthologs in *C. briggsae* (CBP33481), *C. remanei* (RP29913) and *C. brenneri* (CN26204), and *C. elegans* IGCM-3 (T02C5.3b) were obtained from WormBase (version WS235). Human (NP_872381.2) and mouse (NP_001018013.1) IZUMO1 sequences were from the National Center for Biotechnology Information (NCBI). This figure was prepared on the basis of the report by Nishimura *et al*. (2015).

Constructs encoding wild-type SPE-45 (IgWT) or chimeric SPE-45, where the SPE-45 Ig-like domain was replaced with the mouse IZUMO1 Ig-like domain (IgIZUMO1), were created (Figure 2.5A). As a control, we created a chimeric construct encoding SPE-45 where the natural Ig-like domain was replaced with that of *C. elegans* IGCM-3 (IgIGCM3) (Figure 2.5A), a somatic protein with no obvious role during fertilization (www.wormbase.org). These three constructs were used to create transgenes that were evaluated for rescue of *spe-45* self-sterility (Figure 2.5A).

In the absence of any transgenes, *spe-45(tm3715)* hermaphrodites were completely sterile (data not shown). Intriguingly, *spe-45* mutant hermaphrodites bearing the IgIZUMO1 or IgIGCM3 (negative control) transgenes had self-broods that were, respectively, ~77% or 0% of those with the IgWT transgene. These data suggest that the Ig-like domains of SPE-45 and IZUMO1 have a common function(s) during sperm-oocyte fusion.

As shown in Figure 2.5B, while the SPE-45 Ig-like domain is well conserved among four *Canorhabditis* species (~75-83% identities), there are only limited

primary sequence identities of the Ig-like domains between *C. elegans* SPE-45 and mouse or human IZUMO1s or *C. elegans* IGCM-3 (~12-17% identities). Therefore, a difference of the rescue activities of IgIZUMO1 and IgIGCM3 was unlikely to be based on the sequence identities of the Ig-like domains among *C. elegans* SPE-45, mouse IZUMO1 and *C. elegans* IGCM-3.

2-2-3 Folate transporter proteins FOLT-2 and FOLT-3 are not essential for fertilization

JUNO is a GPI-anchored folate receptor-like protein that acts as an IZUMO1 receptor on the oocyte surface (Bianchi et al., 2014). Although perhaps this protein is functionally independent of folate (Bianchi et al., 2014), the author examined a possibility that a folate-related protein(s) might be involved during *C. elegans* gamete fusion. In *C. elegans*, genes that encode GPI-anchored folate receptor-like proteins (mouse *Juno*-like genes) have not been yet found (Garyson, 2015), but there are the folate transporter genes *folt-1*, *folt-2* and *folt-3*. While *folt-1* is involved in folate-related biological events that are presumably independent of reproduction (Austin et al., 2010), functions of *folt-2* and *folt-3* are currently unknown. Thus, the author created worms in which either *folt-2* or *folt-3* genes are mutated by clustered regularly interspaced short palindromic repeat (CRISPR)/CRISPR-associated protein 9 (Cas9), and the self-fertility of those mutants was examined.

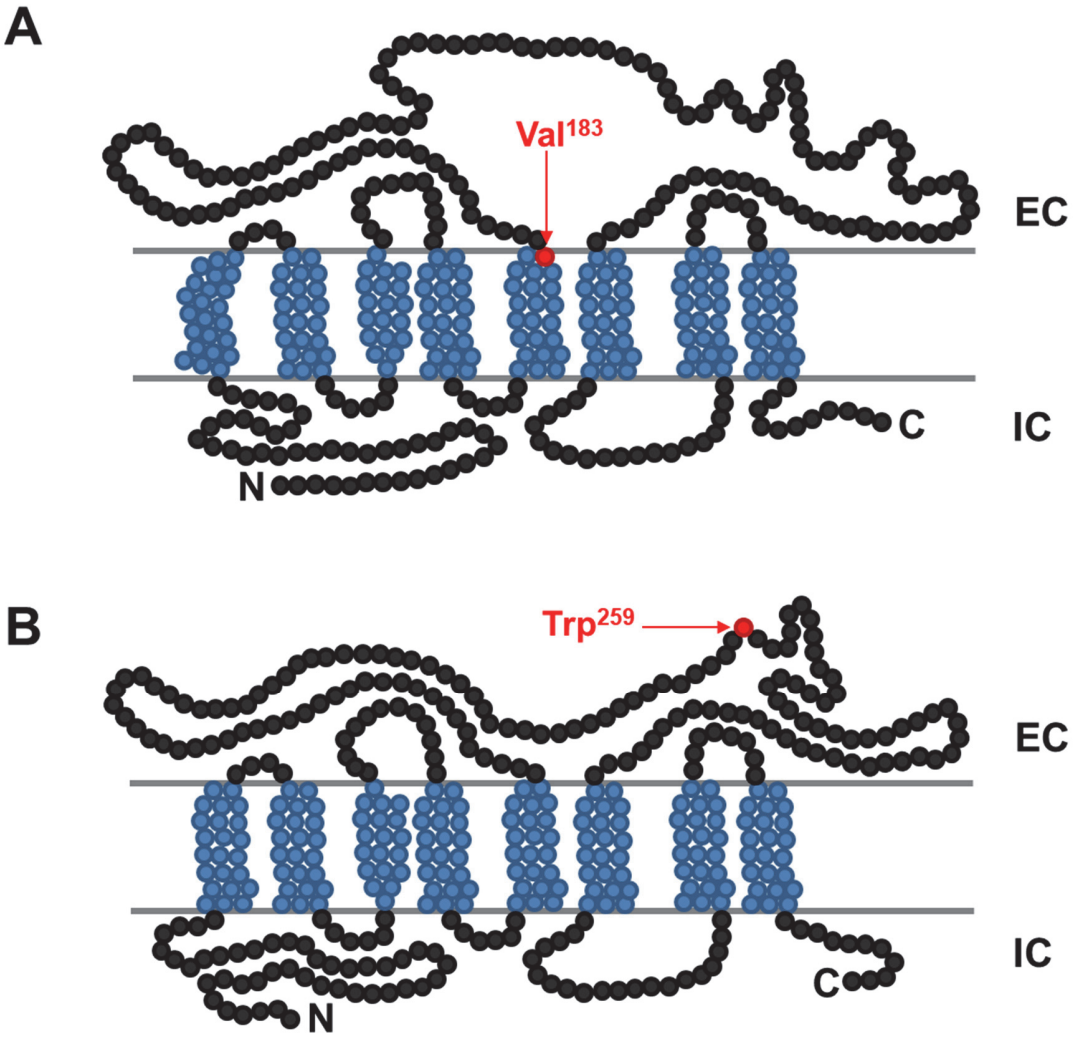

Figure 2.6 Structures of *C. elegans* FOLT-2 and FOLT-3 proteins. (A) FOLT-2 protein (424 aa). A translated protein from *folt-2(nyg1)* gene seems to lack a 9-aa stretch of which the first residue is Val^{183} (indicated by a red arrow). (B) FOLT-3 protein (424 aa). A reading frame is shifted from a codon corresponding to Trp^{259} in *folt-3(nyg2)* gene (indicated by a red arrow), causing an immature termination of protein synthesis of FOLT-3. EC, extracellular; IC, intracellular; N, N-terminus; C, C-terminus.

As CRSPR/Cas9 targeted *folt-2* gene, 27 nucleotides were deleted from the third exon (hereafter the deletion allele was named *nyg1*). This seems to cause

a lack of a 9-aa stretch (Val[183]-Glu-Trp-Lys-Glu-Ala-Tyr-Glu-Lys[191]) in FOLT-2 protein (Figure 2.6A). *folt-3* gene was also targeted by CRISPR/Cas9, resulting in a deletion of seven nucleotides from the fifth exon (hereafter the deletion allele was named *nyg2*). The frameshift mutation likely causes an immature termination of FOLT-3 synthesis (Figure 2.6B), suggesting that a protein translated from *folt-3(nyg2)* is lacking or non-functional in worms.

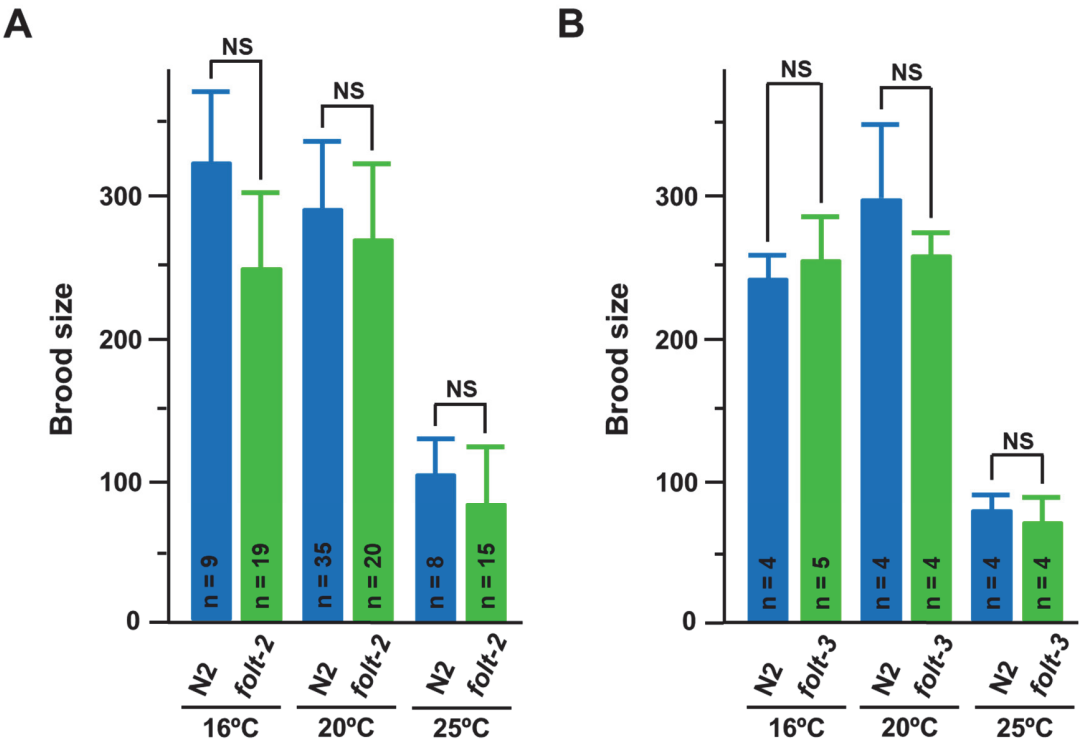

Figure 2.7 *C. elegans folt-2(nyg1)* and *folt-3(nyg2)* hermaphrodites are normally fertile. Self-brood sizes (number of self-progeny) of *folt-2(nyg1)* (A) and *folt-3(nyg2)* (B) hermaphrodites were examined at 16, 20 and 25ºC. As controls, brood sizes of wild-type hermaphrodites (N2) were also examined. The data are shown as mean ± SEM. NS, not significant.

The author examined the self-fertility of *folt-2(nyg1)* and *folt-3(nyg2)* hermaphrodites at 16, 20 and 25ºC (Figure 2.7B). However, no mutants exhibited the self-sterility at any tested temperatures, indicating that self-fertilization normally occurred in *folt-2(nyg1)* and *folt-3(nyg2)* worms. Thus, perhaps FOLT-2 and FOLT-3 proteins are dispensable for fertilization, and it is unlikely that either or both of these two proteins act as a SPE-45 receptor.

2-3 Discussion

In general, genes that act in reproduction evolve more rapidly than somatic genes, making it challenging to identify orthologs of such reproduction-related genes by BLAST-based searches. For instance, past gene-targeting studies showed that the mouse *Adam1a* (Nishimura et al., 2004) and *Adam3* (Shamsadin et al., 1999; Nishimura et al., 2001) genes are indispensably required for male fertility, but their human orthologs predicted by homology searches are non-functional as pseudogenes (Jury et al., 1997; Grzmil et al., 2001). Therefore, it is largely unclear whether the mechanisms for reproduction-related phenomena, including gamete fusion, are conserved between evolutionarily distant species.

Nishimura *et al.* (2015) postulated that the *C. elegans* genome encodes an ortholog of the mouse *Izumo1* gene as a member of the *spe-9* class. They eventually identified *spe-45* gene by a reverse genetic approach, but the gene was dispensable for spermatogenesis (spermatid production *via* meiosis) and spermiogenesis (spermatid activation into spermatozoa). Hence, in this study, the author examined if *spe-45* acts during fertilization (almost equal to gamete fusion in *C. elegans*).

The author employed a time-lapse analysis to test the ability of *spe-45(tm3715)* spermatozoa to fertilize oocytes; it is to count the number of self-sperm in the spermatheca of *spe-45(tm3715)* hermaphrodites (Figure 2.4,Table 2.2). This analysis is an indirect way to know if fertilization occurs, but it provides useful information for how *spe-9* class genes are involved during

gamete fusion. The data on Figure 2.4 and Table 2.2 suggest that *spe-9* and *spe-45* mutant spermatozoa presumably have defects in later steps during gamete fusion, while those mutant spermatozoa seem to be capable of binding to the oocyte PM. Contrarily, *spe-42* likely acts in an initial step during gamete fusion, such as binding of spermatozoa to the oocyte PM.

It is worth to note that there is another possible interpretation for the time-lapse data; *spe-9* and/or *spe-45* might act in sperm guidance. Relevant to Figure 2.3A, in wild type, spermatozoa that are not consumed by fertilization are pushed from the spermatheca into the uterus, accompanying fertilized oocytes (*spe-9* class mutant self-sperm will accompany unfertilized oocytes, see Figure 2.3B). Then, the spermatozoa in the uterus crawl back into the spermatheca. When genes that are involved in synthesis of F-series prostaglandins from yolk lipoprotein complex-derived unsaturated fatty acids are mutated, spermatozoa become partly defective in their relocation from the uterus into the spermatheca (Kubagawa et al., 2006; Hoang et al., 2013; McKnight et al., 2014). These phenotypes seem similar to those of *spe-9* and *spe-45* mutants, resulting in the incomplete sperm recruitment into the spermatheca. Currently, the sperm prostaglandin receptor(s) is not known, but SPE-9 and/or SPE-45 could function in the prostaglandin binding to spermatozoa and/or subsequent sperm reaction(s).

The author further examined if SPE-45 and IZUMO1 are functionally related to each other (Figure 2.5A). A transgene was constructed encoding chimeric SPE-45, where the native Ig-like domain was removed and replaced by the mouse IZUMO1 Ig-like domain (IgIZUMO1). When the transgene was

expressed in *spe-45(tm3715)* hermaphrodites, the self-sterility of the mutant was rescued to ~77% of the level observed for the wild-type transgene (IgWT). This finding suggests that the Ig-like domains of SPE-45 and IZUMO1 share a common function that has been conserved during evolution for ~900 million years (Blaxter, 2009).

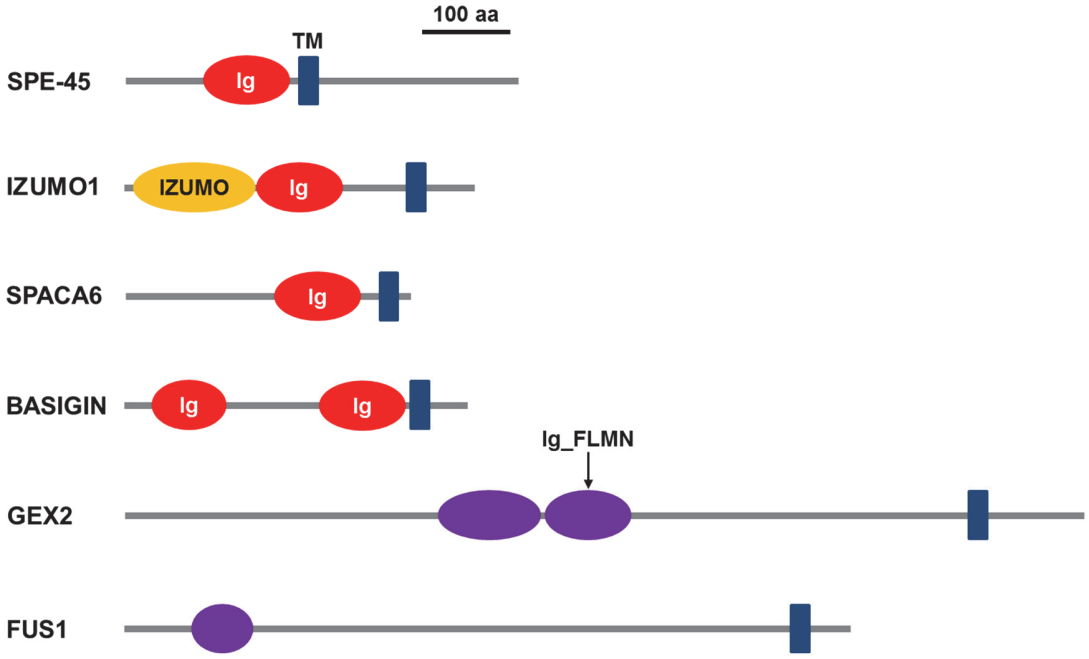

Figure 2.9 Domain architectures of Ig-like TM proteins that are involved during gamete interactions in diverged organisms. TM proteins shown here are from a variety of species, contain the Ig-like or Ig-like folded filamin (Ig_FLMN) domains, and play important roles in gamete interactions. IZUMO1 possesses the IZUMO domain, in addition to the Ig-like and the TM domains. A black bar represents a 100-aa stretch. This figure was prepared on the basis of the review by Nishimura & L'Hernault (2016).

However, the functional roles that are played by the Ig-like domains in *C. elegans* SPE-45 and mouse IZUMO1 are currently unknown. Intriguingly,

besides these two proteins, other Ig-like TM proteins that are originated from a variety of organisms have been found to participate in gamete interactions (Figure 2.9). The mutant mouse line BART97b, in which the *Spaca6* gene encoding an Ig-like TM protein is lacking, produces spermatozoa that cannot fuse with the oocyte PM (Lorenzetti et al., 2014). Another example in the mouse is the *Bsg* gene that encodes a single-pass TM protein containing two Ig-like domains. Male and female *Bsg*-knockout mice are both sterile, and spermatogenesis is arrested in males (Igakura et al., 1998). Later study showed that the BSG protein is also involved during sperm interactions with the CL and the ZP (Saxena et al., 2002). *Arabidopsis* and *Chlamydomonas* have GEX2 (Mori et al., 2014; Mori & Igawa, 2014) and FUS1 (Ferris et al., 1996; Misamore et al., 2003), respectively, both of which are single-pass TM proteins with Ig-like filamin repeat domains. These two proteins act in gamete fusion or attachment.

As in the case of SPE-45 and IZUMO1, it remains clarified how Ig-like domains found in the mouse, plant and algal proteins are involved in gamete interactions. The *Hydractinia* Alr1 and Alr2 genes might provide clues to the functions of Ig-like domains during fertilization, although perhaps these two genes are dispensable for gamete interactions. Alr1 and Alr2 genes encode TM proteins with multiple Ig-like domains that play critical roles in recognition of self- *versus* non-self (allo-recognition) through *trans*-homotypic interactions of Alr proteins (Karadge et al., 2015). The other Ig-like TM proteins shown in Figure 2.9, like the Alr proteins, possibly associate with the same and/or other TM proteins containing Ig-like domains to form *cis*- and/or *trans*-protein

complexes that are important for fertilization. For example, on the mouse sperm surface, IZUMO1 and SPACA6 might interact to each other, although any functional relationship between these two mouse proteins is presently unclear. Since, besides *spe-45*, *C. elegans* has genes encoding Ig-like TM proteins with specific or predominant expression in either male or female germlines (Nishimura et al., 2015), there might be a SPE-45 partner(s) with such the domain architecture on the surface of spermatozoa and/or oocytes.

Another aspect to consider the functional relationship of SPE-45 and IZUMO1 is that mouse JUNO, a GPI-anchored folate receptor-like protein, is an IZUMO1 receptor on the oocyte surface. The IZUMO1-JUNO protein complex is prerequisite for sperm-oocyte fusion in mice, and the IZUMO domain of IZUMO1 (Figure 2.9) is indispensable for the protein complex formation (Inoue et al., 2013; Bianchi et al., 2014; Inoue et al., 2015). Moreover, Inoue *et al.* (2015) suggested the presence of a secondary IZUMO1 receptor on the oocyte surface that possibly acts after IZUMO1 binding to JUNO. Therefore, SPE-45's Ig-like domain might indirectly act in binding to an oocyte SPE-45 receptor or participate in a later step(s) after the primary ligand-receptor binding during gamete fusion. It seems probable that the SPE-45, like IZUMO1, interacts with a receptor on the oocyte surface and, perhaps, the Ig-like domain plays a role.

Since *C. elegans* seems to have no genes encoding mouse JUNO-like proteins (Grayson, 2015), the author postulated that folate-related proteins such as *C. elegans* FOLT proteins (Figure 2.6) might be alternative candidates of the oocyte-resident receptor for SPE-45. The author created *C. elegans* strains carrying mutations in either *folt-2* or *folt-3* genes and examined their self-fertility,

because these two genes encode folate transporter proteins with unknown functions. As shown in Figure 2.7, *folt-2(nyg1)* and *folt-3(nyg2)* hermaphrodites both exhibited normal brood sizes, suggesting that self-fertilization normally occurred in these mutants. Thus, it is still unknown yet whether or not SPE-45 is functionally related to a certain oocyte-surface protein(s). To elucidate the precise role of SPE-45, identification of its *cis*- (on the sperm surface) and/or *trans*- (on the oocyte surface) partners will provide key insights.

2-4 Experimental procedures

2-4-1 Worm strains

We maintained and cultured worms at 20ºC, unless otherwise stated, according to standard methods (Brenner, 1974). *C. elegans* var. Bristol (N2) or *him-5(e1490)V* (DR466) worms were used as wild-type/control strains. *spe-42(tm2421)V* and *spe-45(tm3715)IV* worms were obtained from the National BioResource Project (NBRP, at Tokyo Women's Medical University, Japan), outcrossed five times with N2 males, and maintained as a heterozygote with the balancer chromosome *nT1[unc-?(n754) let-? qIs50]IV;V* (Ferguson & Horvitz, 1985). *spe-9(eb19)I; him-5(e1490)V; ebEx126[spe-9(+) + rol-6(su1006)]* (SL438) was also used in this study. All strains used in this study except for the *spe-42* and *spe-45* mutants were from the *Caenorhabditis* Genetic Center (CGC, at the University of Minnesota, USA).

2-4-2 Cloned DNAs

pMW118, pPD118.20 (used as a transgene encoding *Pmyo-3::GFP*) and pCXN2 carrying mouse *Izumo1* cDNA were provided by Drs. Takeshi Ishihara (Kyushu University, Japan), Andrew Fire (Stanford University, USA) and Masaru Okabe (Osaka University, Japan), respectively. The fosmid DNA WRM062dB01, containing *spe-45* (*F28D1.8*) gene, was obtained from the Wellcome Trust Sanger Institute (UK), and it was used to be expressed in *spe-45(tm3715); him-5(e1490)* worms for maintenance of this strain. pCFJ104 (used as a transgene encoding *Pmyo-3::mCherry*) and pDD162 (used for gene targeting by

CRISPR/Cas9) were provided from Addgene (USA).

2-4-3 PCR primers

Below are the sequences of PCR primers used in this study.

HN086: GCCCTTTGCCTTACTCTCAAT

HN095: GCCTCGAGACAACCTCTAATTGAAAATGAGGC

HN109: ACTGAGCAGACATTTGAAAGTCACCATTGT

HN110: ACTTTCAAATGTCTGCTCAGTTGGCATCGT

HN111: ATTTGACAGACAGCGGTAGTTGCCAGCATC

HN112: AACTACCGCTGTCTGTCAAATGGACAGCTC

HN150: CAACCTCGCATTTGAAAGTCACCATTGTACCG

HN151: GACTTTCAAATGCG GGTTGAGGGAAATCC

HN156: CATTTGACAGACACCAGTATTGTCCGGAATA

HN157: ATACTGGTGTCTGTCAAATGGACAGCTCATT

HN190: TACAGCTCTCACCACTGATTCC

STNHN76: CAAGACATCTCGCAATAGG

STNHN179: CTTCCTTCCACTCAACACCGTTTTAGAGCTAGAAATAGCAAG

STNHN180: 5CGCCATGACAATTGCGGTAT

STNHN181: CGAAAGAGCCGACCAAACAG

STNHN182: TTGGCTCCCTGCTACAAGCGTTTTAGAGCTAGAAATAGCAAGT

STNHN183: GTTCCATTGCTCGGAATCCC’

STNHN184: CCCGAACAACCGTGAATCAA

2-4-4 PCR

All PCRs were carried out using the Advantage cDNA Polymerase Mix (Clontech). PCR products were cloned into pCR-Blunt II (Life Technologies), their DNA sequences were verified (Eurofins Genomics), and the inserts were subcloned into desired plasmids for use in further experiments.

2-4-5 Microscopy

Most worm handling, such as picking, counting and dissecting, were carried out under SZ61 or SZX10 dissecting microscopes (Olympus). To capture digital images of cells, tissues and worms, we used a BX60 microscope (Olympus) equipped with a SensiCam CCD camera (Cooke) using Image-Pro PLUS (Media Cybernetics) and VolumeScan 3.1 (VayTek) softwares. For the same purpose, we also adopted an Olympus BX53 microscope carrying a DP72 CCD camera with cellSens software (Olympus). Microinjections were performed under an IX73 microscope (Olympus) equipped with a manipulator set of MN-4, MO-202U and MNO-220A (Narishige) and with FemtJet Express (Eppendorf).

2-4-6 Fertilization assay

L4 hermaphrodites that were either N2, *him-5(e1490)*, *spe-9(eb19); him-5(e1490)*, *spe-42(tm2421)* or *spe-45(tm3715)* were incubated at 20ºC. After 24 and 72 h, animals were fixed for 10 min in 0.1 M K_2HPO_4 containing 3% paraformaldehyde, followed by 5-min incubation in -20ºC methanol, washed with phosphate-buffered saline containing 0.1% Tween 20, mounted in Prolong Gold with DAPI (Molecular Probes), and observed under the BX60 or BX63

microscopes to determine whether self-sperm either persisted or were successively diminished in numbers because they participated in fertilization occurring in the spermatheca. Deconvolution microscopy was used to recover a Z-stack of images from one spermatheca/hermaphrodite. The Z stack was flattened to create a projection image, all self-sperm were counted and, when necessary, individual sections were examined to ensure that no sperm were missed.

2-4-7 Cloning of spe-45

A genomic fragment including the *spe-45* gene and its native 5'- and 3'-flanking regions, both of which extend up to but not into the neighboring genes, was cloned into pMW118. A 5' DNA fragment was amplified by PCR using HN95 and HN190 as primers and the fosmid clone WRM062dB01 as a template. To obtain a 3' DNA fragment, the fosmid clone WRM062dB01 was digested with *BamH I*. The 5' and 3' fragments were then ligated together into a pMW118 vector to construct the final plasmid (IgWT/pMW118, Figure 2.5A). The composite insert was ~4.8 kbp in length and could be excised by double restriction digestions with *Xho I* and *Sal I*.

2-4-8 Construction of chimeric SPE-45 containing different Ig-like domains

For both the *spe-45*/*Izumo1* (IgIZUMO1, Figure 2.5A) and the *spe-45*/*igcm-3* (IgIGCM3, Figure 2.5A) chimeric constructs, a PCR strategy was used to create a single construct composed of the 5'-flanking region (including the *spe-45* promoter sequence), either of the two chimeric genes, and the 3'-flanking region.

A ~3.6-kbp DNA fragment corresponding to the 3' *spe-45* region that was common to both the chimeric constructs was obtained by restriction digestion of IgWT/pMW118. The 5' regions for each construct were prepared as described below.

2-4-8-1 spe-45/*Izumo1*

The 5' fragment of the *spe-45*/*Izumo1* chimeric construct that included the Ig-like loop region of mouse *Izumo1* cDNA was prepared using four PCR reactions (PCR1-4), as shown below.

PCR No.	Primer set	Template DNA
PCR1	HN95 and HN109	WRM062dB01
PCR2	HN110 and HN111	Mouse *Izumo1* cDNA
PCR3	HN112 and HN86	WRM062dB01
PCR4	HN95 and HN86	Mix of PCR1, PCR2 and PCR3

The 5' DNA fragment was released from the PCR4 DNA product by restriction digestion and then ligated with the common 3' DNA fragment into pMW118.

2-4-8-2 spe-45/*igcm-3*

The 5' fragment of the *spe-45*/*igcm-3* chimeric construct that included the Ig-like loop region of *C. elegans igcm-3* cDNA was prepared using four PCR reactions (PCR5-8), as shown below. To prepare *C. elegans* total cDNA used for PCR6,

total RNA was extracted from adult N2 worms using TRIzol (Life Technologies). Then, the first strand cDNA was synthesized from the RNA preparation and random primers by using the Advantage RT-for-PCR Kit (Clonthech), according to the manufacturer's protocol.

PCR No.	Primer set	Template DNA
PCR5	HN95 and HN150	WRM062dB01
PCR6	HN151 and HN156	*C. elegans* total cDNA
PCR7	HN157 and HN86	WRM062dB01
PCR8	HN95 and HN86	Mix of PCR5, PCR6 and PCR7

As described above, the 5' DNA of *spe-45*/*igcm-3* was prepared and then ligated with the common 3' DNA fragment.

2-4-9 Rescue assay

The insert DNA fragments (~4.8 kbp) were released by double restriction digestion with *Xho I* and *Sal I* from either IgWT/pMW118, IgIZUMO1/pMW118 or IgIGCM3/pMW118. pPD118.20, which encodes a GFP marker exclusively for muscle cells, was linearized by digestion with *Sca I*. Genomic DNA was isolated from adult N2 worms and digested with *Pvu II* in the presence of ribonuclease A (Sigma-Aldrich). Since *spe-45* has a *Pvu II* site, isolated N2 genomic DNA was extensively digested with this restriction enzyme to destroy all intact copies of the *spe-45* gene.

The author prepared a solution containing 1 ng/μl linearized pPD118.20, 97 ng/μl *Pvu II*-digested N2 genomic DNA and 2 ng/μl one of the *spe-45* inserts, and this DNA mixture was microinjected into young adult *him-5(e1490)* hermaphrodites to create what are termed complex arrays (Kelly et al., 1997). Then, GFP-positive male progeny mated with *spe-45(tm3715); him-5(e1490)* hermaphrodites to produce rescue strains expressing either IgWT, IgIZUMO1 or IgIGCM3 in the *spe-45* mutant.

The number of self-progeny produced by transgenic hermaphrodites bearing the IgWT, IgIZUMO1 and IgIGCM3 transgenes was then determined to evaluate whether the Ig-like domain of SPE-45 plays a role(s) during fertilization. As a negative control, we also tested complex arrays composed of *Pvu II*-cut N2 genomic DNA and pPD118.20 but lacking any of the above-discussed *spe-45* inserts and found that they did not rescue the self-sterility of *spe-45* mutant worms (data not shown).

2-4-10 Creation and fertility assay of folt-2 and folt-3 mutants

Target sequences within exons of *folt-2* and *folt-3* genes were searched by the web tool “CRISPR Optimal Target Finder” (http://tools.flycrispr.molbio.wisc.edu/targetFinder/index.php). DNA fragments corresponding to single guide RNA (sgRNA) sequences for targeting of *folt-2* and *folt-3* were introduced into pDD162 by using the Q5 Site-Directed Mutagenesis Kit (New England Biolabs), in order to produce the CRISPR/Cas9 plasmids folt2_sgRNA/pDD162 and folt3_sgRNA/pDD162.

DNA solutions containing 30 ng/μl pCFJ104 and 70 ng/μl

folt2_sgRNA/pDD162 or folt3_sgRNA/pDD162 were microinjected to young adult N2 hermaphrodites. To screen worms carrying deletions in either *folt-2* or *folt-3* genes, single worm PCR was performed. Candidate worms were individually put into 1.5-ml tubes containing 20 μl of 1 x PCR buffer containing 1 mg/ml Proteinase K (Life Technologies). A cycle of freezing at -80ºC and thawing at room temperature was repeated three times, followed by incubation at 60ºC for 1 h and subsequently at 100ºC for 15 min. The genomic DNA samples were added to PCR reaction mixtures (10% volume of total), containing a primer set of STNHN180 and STNHN181 for *folt-2* gene or STNHN183 and STNHN184 for *folt-3* gene. The resulting PCR products were analyzed by 2% agarose gel electrophoresis and DNA sequencing.

Eventually *folt-2(nyg1)* and *folt-2(nyg2)* worms, both of which homozygously carried deletion alleles, were obtained. Then, numbers of self-progeny were counted for *folt-2(nyg1)* and *folt-2(nyg)* worms at 16, 20 and 25ºC.

References

Bianchi, E., Doe, B., Goulding, D., & Wright, G. J. (2014). Juno is the egg Izumo receptor and is essential for mammalian fertilization. *Nature*, *508*(7497), 483-487. doi: 10.1038/nature13203

Bork, P., Holm, L., & Sander, C. (1994). The immunoglobulin fold. Structural classification, sequence patterns and common core. *Journal of Molecular Biolology*, *242*(4), 309-320.

Brenner, S. (1974). The genetics of Caenorhabditis elegans. *Genetics*, *77*(1), 71-94.

Chatterjee, I., Richmond, A., Putiri, E., Shakes, D. C., & Singson, A. (2015). The Caenorhabditis elegans spe-38 gene encodes a novel four-pass integral membrane protein required for sperm function at fertilization. *Development*, *132*(12), 2795-2808.

Ferguson, E. L., & Horvitz, H. R. (1985). Identification and characterization of 22 genes that affect the vulval cell lineages of the nematode Caenorhabditis elegans. *Genetics*, *110*(1), 17–72.

Ferris, P. J., Woessner, J. P., & Goodenough, U. W. (1996). A sex recognition glycoprotein is encoded by the plus mating-type gene fus1 of Chlamydomonas reinhardtii. *Molecular Biology of the Cell*, *7*(8), 1235-1248.

Florman, H. M., & Fissore, R. A. (2015). Fertilization in mammals. *Knobil and Neill's Physiology of Reproduction* (4th ed.), Cambridge, MA: Academic Press, 149-196. https://doi.org/10.1016/B978-0-12-397175-3.00004-1

Grayson, P. (2015). Izumo1 and Juno: the evolutionary origins and coevolution

of essential sperm-egg binding partners. *Royal Society Open Science*, *2*(12), 150296. https://doi.org/10.1098/rsos.150296

Grzmil, P., Kim, Y., Shamsadin, R., Neesen, J., Adham, I. M., Heinlein, U. A., Schwarzer, U. J., & Engel, W. (2001). Human cyritestin genes (CYRN1 and CYRN2) are non-functional. *Biochemical Journal*, *357*(Pt 2), 551-556.

Haerty, W., Jagadeeshan, H., Kulathinal, R. J., Wong, A., Ravi Ram, K., Sirot, L. K., Levesque, L., Artieri, C. G., Wolfner, M. F., Civetta, A., & Singh, R. S. (2007). Evolution in the fast lane: rapidly evolving sex-related genes in Drosophila. *Genetics*, *177*(3), 1321-1335.

Halaby, D. M., Poupon, A., & Mornon, J. P. (1999). The immunoglobulin fold family: sequence analysis and 3D structure comparisons. *Protein Engineering*, *12*(7), 563-571.

Hoang, H. D., Prasain, J. K., Dorand, D., & Miller, M. A. (2013). A heterogeneous mixture of F-series prostaglandins promotes sperm guidance in the Caenorhabditis elegans reproductive tract. *PLoS Genetics*, *9*(1), e1003271. doi: 10.1371/journal.pgen.1003271

Igakura, T., Kadomatsu, K., Kaname, T., Muramatsu, H., Fan, Q. W., Miyauchi, T., To-yama, Y., Kuno, N., Yuasa, S., Takahashi, M., Senda, T., Taguchi, O., Yamamura, K., Arimura, K., & Muramatsu, T. (1998). A null mutation in basigin, an immunoglobulin superfamily member, indicates its important roles in peri-implantation develop-ment and spermatogenesis. *Developmental Biology*, *194*(2), 152-165.

Inoue, N., Ikawa, M., Isotani, A., & Okabe, M. (2005). The immunoglobulin superfamily protein Izumo is required for sperm to fuse with eggs. *Nature*,

434(7030), 234-238.

Inoue, N., Hamada, D., Kamikubo, H., Hirata, K., Kataoka, M., Yamamoto, M., Ikawa, M., Okabe, M., & Hagihara, Y. (2013). Molecular dissection of IZUMO1, a sperm protein essential for sperm-egg fusion. *Development*, *140*(15), 3221-3229. doi: 10.1242/dev.094854

Inoue, N., Hagihara, Y., Wright, D., Suzuki, T., & Wada, I. (2015). Oocyte-triggered dimeri-zation of sperm IZUMO1 promotes sperm-egg fusion in mice. *Nature Communication*, *6*, 8858. doi: 10.1038/ncomms9858

Jury, J. A., Frayne, J., & Hall, L. (1997). The human fertilin alpha gene is non-functional: implications for its proposed role in fertilization. *Biochemical Journal*, *321*(Pt 3), 577-581.

Kelly, W. G., Xu, S. Q., Montgomery, M. K., & Fire, A. (1997). Distinct requirements for somatic and germline expression of a generally expressed Caenorhabditis elegans gene. *Genetics*, *146*(1), 227-238.

Kroft, T. L., Gleason, E. J., & L'Hernault, S. W. (2005). The spe-42 gene is required for sperm-egg interactions during C. elegans fertilization and encodes a sperm-specific transmembrane protein. *Developmental Biology*, *286*(1), 169-181.

Kubagawa, H. M., Watts, J. L., Corrigan, C., Edmonds, J. W., Sztul, E., Browse, J., & Miller, M. A. (2006). Oocyte signals derived from polyunsaturated fatty acids control sperm recruitment in vivo. *Nature Cell Biology*, *8*(10), 1143-1148.

L'Hernault, S. W., Shakes, D. C., & Ward, S. (1988). Developmental genetics of chromosome I spermatogenesis-defective mutants in the nematode Caenorhabditis elegans. *Genetics*, *120*(2), 435-452.

Lorenzetti, D., Poirier, C., Zhao, M., Overbeek, P. A., Harrison, W., & Bishop, C. E. (2014). A transgenic insertion on mouse chromosome 17 inactivates a novel immunoglobulin superfamily gene potentially involved in sperm-egg fusion. *Mammalian Genome*, *25*(3-4), 141-148. doi: 10.1007/s00335-013-9491-x

Marcello, M. R., Singaravelu, G., & Singson, A. (2013). Fertilization. *Advances in Experimental Medicine and Biology*, *757*, 321-350. doi: 10.1007/978-1-4614-4015-4_11

McKnight, K., Hoang, H. D., Prasain, J. K., Brown, N., Vibbert, J., Hollister, K. A., Moore, R., Ragains, J. R., Reese, J., & Miller, M. A. (2014). Neurosensory perception of environmental cues modulates sperm motility critical for fertilization. *Science*, *344*(6185), 754-757. doi: 10.1126/science

Miller, M. A., Nguyen, V. Q., Lee, M. H., Kosinski, M., Schedl, T., Caprioli, R. M., & Greenstein, D. (2001). A sperm cytoskeletal protein that signals oocyte meiotic maturation and ovulation. *Science*, *291*(5511), 2144-2147.

Misamore, M. J., Gupta, S., & Snell, W. J. (2003). The Chlamydomonas Fus1 protein is present on the mating type plus fusion organelle and required for a critical mem-brane adhesion event during fusion with minus gametes. *Molecular Biology of the Cell*, *14*(6), 2530-2542.

Mori, T., Igawa, T., Tamiya, G., Miyagishima, S. Y., & Berger, F. (2014). Gamete attach-ment requires GEX2 for successful fertilization in Arabidopsis. *Current Biology*, *24*(2), 170-175. doi: 10.1016/j.cub.2013.11.030

Mori, T., & Igawa, T. (2014). Gamete attachment process revealed in flowering plant fertilization. *Plant Signaling & Behavior*, *9*(12), e977715. doi:

10.4161/15592324.2014.977715

Nelson, G. A., Lew, K. K., & Ward, S. (1978). Intersex, a temperature-sensitive mutant of the nematode Caenorhabditis elegans. *Developmental Biology*, *66*(2), 386-409.

Nishimura, H., Cho, C., Branciforte, D. R., Myles, D. G., & Primakoff, P. (2001). Analysis of loss of adhesive function in sperm lacking cyritestin or fertilin beta. *Developmental Biology*, *233*(1), 204-213.

Nishimura, H., Kim, E., Nakanishi, T., & Baba, T. (2004). Possible function of the ADAM1a/ADAM2 Fertilin complex in the appearance of ADAM3 on the sperm surface. *Journal of Biological Chemistry*, *279*(33), 34957-34962.

Nishimura, H., & L'Hernault, S. W. (2010). Spermatogenesis-defective (spe) mutants of the nematode Caenorhabditis elegans provide clues to solve the puzzle of male germline functions during reproduction. *Developmental Dynamics*, *239*(5), 1502-1514. https://doi: 10.1002/dvdy.22271

Nishimura, H., Tajima, T., Comstra, H. S., Gleason, E. J., & L'Hernault, S. W. (2015). The immunoglobulin-like gene spe-45 acts during fertilization in Caenorhabditis elegans like the mouse Izumo1 gene. *Current Biology*, *25*(24), 3225-3231. https://doi: 10.1016/j.cub.2015.10.056

Nishimura, H., & L'Hernault, S. W. (2016). Gamete interactions require transmembranous immunoglobulin-like proteins with conserved roles during evolution. *Worm*, *5*(3), e1197485.

Putiri, E., Zannoni, S., Kadandale, P., & Singson, A. (2004). Functional domains and temperature-sensitive mutations in SPE-9, an EGF repeat-containing

protein required for fertility in Caenorhabditis elegans. *Developmental Biology*, *272*(2), 448-459.

Saxena, D. K., Oh-Oka, T., Kadomatsu, K., Muramatsu, T., & Toshimori, K. (2002). Behaviour of a sperm surface transmembrane glycoprotein basigin during epididymal maturation and its role in fertilization in mice. *Reproduction*, *123*(3), 435-444.

Shamsadin, R., Adham, I. M., Nayernia, K., Heinlein, U. A., Oberwinkler, H., & Engel, W. (1999). Male mice deficient for germ-cell cyritestin are infertile. *Biology of Reproduction*, *61*(6), 1445-1451

Singaravelu, G., Chatterjee, I., Rahimi, S., Druzhinina, M. K., Kang, L., Xu, X. Z., & Singson, A. (2012). The sperm surface localization of the TRP-3/SPE-41 Ca^{2+}-permeable channel depends on SPE-38 function in Caenorhabditis elegans. *Developmental Biology*, *365*(2), 376-383. doi: 10.1016/j.ydbio.2012.02.037

Singaravelu, G., Rahimi, S., Krauchunas, A., Rizvi, A., Dharia, S., Shakes, D., Smith, H., Golden, A., & Singson, A. (2015). Forward genetics identifies a requirement for the Izumo-like immunoglobulin superfamily spe-45 gene in Caenorhabditis elegans fertilization. *Current Biology*, *25*(24), 3220-3224. doi: 10.1016/j.cub.2015.10.055

Singson, A., Mercer, K. B., & L'Hernault, S. W. (1998). The C. elegans spe-9 gene encodes a sperm transmembrane protein that contains EGF-like repeats and is required for fertilization. *Cell*, *93*(1), 71-79.

Swanson, W. J., & Vacquier, V. D. (2002). The rapid evolution of reproductive proteins. *Nature Reviews. Genetics*, *3*(2), 137-144.

Takayama, J., & Onami, S. (2016). The sperm TRP-3 channel mediates the onset of a Ca^{2+} wave in the fertilized C. elegans oocyte. *Cell Reports*, *15*(3), 625-637. doi: 10.1016/j.celrep.2016.03.040

Ward, S., & Carrel, J. S. (1979). Fertilization and sperm competition in the nematode Caenorhabditis elegans. *Developmental Biolology*, *73*(2), 304-321.

Wilson, L. D., Obakpolor, O. A., Jones, A. M., Richie, A. L., Mieczkowski, B. D., Fall, G. T., Hall, R. W., Rumbley, J. N., & Kroft, T. L. (2018). The Caenorhabditis elegans spe-49 gene is required for fertilization and encodes a sperm-specific transmembrane protein homologous to SPE-42. *Molecular Reproduction and Development*, *85*(7), 563-578. doi: 10.1002/mrd.22992

Wyckoff, G. J., Wang, W., & Wu, C. I. (2007). Rapid evolution of male reproductive genes in the descent of man. *Nature*, *403*(6767), 304-309.

Zannoni, S., L'Hernault, S. W., & Singson, A. W. (2003). Dynamic localization of SPE-9 in sperm: a protein required for sperm-oocyte interactions in Caenorhabditis elegans. *BMC Developmental Biology*, *3*, 10.

Xu, X. Z., & Sternberg, P. W. (2003). A C. elegans sperm TRP protein required for sperm-egg interactions during fertilization. *Cell*, *114*(3), 285-297.